Response to referees' comments on:
On the information content in linear horizontal gradients estimated from space geodesy observations

by Gunnar Elgered, Tong Ning, Peter Forkman, and Rüdiger Haas

Introduction

We appreciate the referees' comments and for the time spent on the manuscript, not only for pointing out where clarifications were needed, and identifying a couple of mistakes, but also for suggesting additional comparisons that we think have made it possible to be more specific in some cases, and less specific in other cases. We first describe the major overall changes in the revised manuscript and then we give responses to the individual comments from the referees.

Overall changes

The original manuscript did not have any equations included. Basic equations for the atmospheric refractivity and the type of gradients assessed in the study are now added in Section 2.

The GPS data from the Onsala site during 2013-2016 were reprocessed using three different elevation cutoff angles, alternative mapping functions for the hydrostatic and wet delays, and with and without elevation dependent weighting. As pointed out by both Referees #1 and #2 the discussion paper by Kacmarik et al. (2018) in AMT had found that an elevation angle cutoff at 3° gave the best agreement for estimated gradients. We were now able to confirm this using water vapour radiometer (WVR) data. This means that the results in Section 5.1 are to a large extent new and the section is expanded, e.g. with two new Tables 6 and 7, and the new Figure 11, showing the total gradient sizes from GPS and WVR and the strong correlation between monthly means of gradient size and ZWD (these issues were suggested to discuss in the referees' comments). As suggested by Referee #2, Figure 12 in the original manuscript was removed.

Also gradients estimated from the WVR data were included in the VLBI comparison in Section 5.2 (for completeness and to confirm to what extent gradients seen by the space geodetic techniques, VLBI and GPS, were of atmospheric origin). We removed the old Figure 15, that showed correlation between VLBI and GPS gradients. We think it caused more confusion than understanding. When we now also added the WVR data it seemed reasonable to summarize these correlation coefficients in a table (Table 8 in the revised manuscript).

When WVR data were added to the 15-day long period of the CONT14 campaign we also included the new Figure 16 of the ECMWF gradients in order to show the impact (which is really small in terms of variability) of the hydrostatic gradients added to the WVR wet gradients. The variability seen in the WVR data during the CONT14 also motivated us to go into more detail presenting the zenith wet delays (new Figures 17 and 18) allowing us to discuss the fact that gradients tend to occur during changes of the air masses above the site.

In the following we deal with each referee's comments one by one. The text is colour coded roughly as follows:
Referees' comments are in black font.
Authors' general responses are in blue text and changes in the manuscript in red text.

Referee #1:

The study of the horizontal variability of the atmosphere is currently of great interest. Linear horizontal delay gradients are considered advanced GNSS meteorology products and it has been proved that they are a powerful tool to identify problems with GNSS data tracking. Although not yet assimilated into NWP models, they are fundamental for the reconstruction of the slant delay and, in turn, in the 3D water vapour fields derived by tomographic inversion of GNSS based slants. The analysis of the causes of the time variability on different time scales, from months to minutes, reported in the manuscript adds new insights in the research area of these advanced GNSS meteorology products. In the manuscript, tropospheric gradients estimated from GPS observations are evaluated with respect to independent techniques as WVR and VLBI and independent data as ECMWF in order to assess their quality. I think it would be interesting in future to repeat the same kind of analysis in other regions. However, I would raise the following issues, which have to be clarified prior to the publication.

1. Mapping functions: GPS and VLBI data are analysed using different mapping functions: VMF1 for GPS and Niell for VLBI. No information about the gradient mapping function is given. I guess that in GPS data processing Bar-Sever et al. (1998) gradient mapping function is used, while in VLBI Chen and Herring (1997) gradient mapping function is applied. Kacmarik et al. (2018) recommend to agree on the gradient mapping function when tropospheric gradients derived from various sources are to be compared, since a systematic effect up to 0.3 mm is observed between Bar-Sever et al. (1998) and Chen and Herring (1997) gradient mapping functions. Having this in mind, I think that information on the gradients mapping function has to be provided in the manuscript and properly discussed.

It is correct that the Bar-Sever gradient mapping function is used in all GPS solutions and that the Chen and Herring mapping function was used in the VLBI solution.

This is now clearly stated in Section 3.

We are aware of that the estimated amplitude of the gradients depend on the gradient mapping function chosen.

In the revised paper, we primarily investigated the impact of several different elevation cutoff angles on the resulting gradients. Mapping functions for gradients were not changed.

2. Elevation cut-off: GPS data are processed at 10° and 20° elevation cut-off angle, while no info is provided for VLBI. Kacmarik et al. (2018) obtained better results using 3° elevation cut-off angle and GPS+GLONASS data. I recommend to process at least 1 GPS station with 3° elevation cut-off angle and evaluate the results. Should geodetic data processed with different cut-off angles depending on the application and on the tropospheric parameter of interest (ZTD or gradient)? A comment on this is really appreciated. The manuscript is within the scope of this special issue.

Kačmařík et al (2018), Sensitivity of GNSS tropospheric gradients to processing options, Ann. Geophys. Discuss., https://doi.org/10.5194/angeo-2018-93

We reprocessed the data obtained from ONSA and ONS1 using elevation cutoff angles of 3°, 10°, and 20° from 2013 to 2016. The resulting gradients were compared to the ones obtained by primarily the WVR in Section 5.1, but the 3° solution also to VLBI gradient results in Section 5.2.

Two new tables with results were added and a short discussion is also added in the Conclusions about an optimum elevation cutoff angle.

Below specific comments.

Introduction Page 2 Line 6. I suggest adding the amount of improvement of multi-GNSS gradients compared to GPS-only gradients.
The following text is added in the revised paper "Using multi-GNSS observations, Li et al. (2015) found a significant increase in the correlation coefficients of gradient to about 0.6 when compared to ECMWF gradients, while the one for the GPS-only is usually below 0.5. In addition, they found that the RMS difference of the gradient is reduced to about 25–35 % by multi-GNSS processing."

Cause of horizontal gradient In the manuscript, the mathematical model used to describe the tropospheric path delay is not reported. This can be added in this section and the title should be changed in 'model and cause of horizontal gradient'.
Done.

Instrumentation and data Page 3 Line 11-12. Complete the sentence 'We compare ...' adding at the end '... with respect to VLBI estimates, WVR and ECMWF data' I suggest adding in the section a table summarizing the characteristics of the instruments used for the evaluation, referring to the specific sub-section for further details.
The sentence was modified, but slightly reformulated because we regard the gradients from all these sources to be estimates. When trying to design a table that would include the important characteristics from each instrument we did not end up with a solution that was sufficiently compact, so no new table was introduced.

GPS In this section, and also somewhere else in the manuscript, the term 'site' is used both referring to a local geographical area or referring to a unique geodetic marker. Please review it and use site for a local geographical area, where one or more geodetic markers are available, and station to indicate a unique geodetic marker at a site. Figure 2.
This makes sense and has been adopted in the manuscript.

You present the sky plot of GPS observation for May 12, 2014. Why did you select this specific day?
We selected this day because we have simultaneous observations from GPS and VLBI and the results for this day are further discussed in the corresponding result section.
This now explicitly pointed out in the caption to the figure.

Gradients during the CONT14 VLBI campaign Figure 14. Add mean and std of the differences (GPS-VLBI), are these values affected by the different gradient mapping function?
In the revised paper, we added Table 8 with mean and standard deviation (plus correlation coefficient) obtained when VLBI gradients are compared to GPS and WVR. Because we did not change the gradient mapping function we refer to Kacmarik et al. (2018) to point out that the estimated gradient amplitude will depend on the mapping function.

Typos
Pag.2 Line 4: delete ')' after VLBI
Corrected

Table 2 replace 'igs_1740.atx' with 'igs08_1740.atx', correct?
Corrected, also noted that igs08_1869.atx was used in the reprocessing of the 4 years of data from the Onsala site.

Pag.22 Line 20: horisontal -> horizontal?
Corrected

Referee #2:

As expressed in the title, the manuscript deals with the information content in linear horizontal tropospheric delay gradients estimated from space geodesy observations, namely GPS and VLBI. The topic of the manuscript is highly actual. In past, the tropospheric delay gradients were estimated mainly for improving horizontal positioning (coordinate repeatability), although it was not always clear that it improved the troposphere modelling as the gradient parameters are highly sensitive to other error sources affecting the data analyses. So far, the gradients were also rarely estimated within an operational troposphere monitoring because the information content was often either too noisy or too much smoothed by low temporal resolution or constraints. The situation is going to change in future when providing advanced tropospheric products on troposphere asymmetry monitoring, in particular with upcoming availability of more satellites from multi-GNSS constellations. Tropospheric delay gradients are also pre-requisite for delivering other products from GNSS such as retrieving slant delays, the reconstruction of three-dimensional refractivity field or generating severe weather event indicators. Attempts for developing assimilation techniques for GNSS-based tropospheric gradients emerged recently when it seems preferred way, compared the utilization of slant delays, due to the better production quality in (near) real-time. In this context, the manuscript contributes to a better understanding of how linear tropospheric delay gradients are able to characterize wet and hydrostatic effects of the neutral atmosphere on space geodetic observation analyses; both in actual situation or in a long-term trends and useable in geodetic, meteorological or climatology applications.

1. Adding brief introduction of the model of calculating gradients from the NWM would be helpful for discussion of results, e.g. gradient mapping function, distribution of raytracing points, elevation angle cut-off.
A description of the calculation of gradients from the NWM was added. However, it is our interpretation of the paper by Boehm and Schuh (2007) that the gradients are calculated using three vertical profiles of pressure, temperature, and humidity, without the use of a gradient mapping function, raytracing, or elevation angle cutoff.

2. Although the manuscript study a comparison of gradients, there are no information about gradient mapping functions used in estimating procedures of different techniques. Kačmařík et al. 2018 (submitted for discussions in ANGEO) showed that gradient mapping function could introduce systematic effects into estimated gradients. Similarly, no information about elevation-dependent weighting (if applied) was given neither for GPS nor VLBI. Please, add these information in corresponding tables or text paragraphs, and whenever useful, consider their impact in discussions as these might be more critical than the other processing settings.
In the revised paper, we added results obtained from comparisons of gradients given by different elevation cutoff angles (3°, 10°, and 20°), weighting and non-weighting, and different mapping functions (NMF and VMF1). Tables 6 and 7 and a corresponding discussion were added.

3. The differences in size of estimated gradients estimated from different techniques are not discussed. These are visible in Figure 9 between GPS and Numerical Weather Model (NWM) and in Figures 11 and 12 for GPS compared to WVR. These could be attributed to various aspects such as used gradient mapping functions, limited resolution of numerical weather model data (ECMWF), observation sampling over the sky or others. Were similar characteristics common to the other stations?
For easier reading, I would also suggest to consider splitting sections 4.2 and, optionally

5.1, into two parts with more specific subtitles for more better clarity of different comparisons, see bellow in specific comments.
The new Figure 11 helps us to discuss the (large) uncertainty in the estimated gradient amplitudes. We use ECMWF mainly to remove the hydrostatic gradients which seems to be possible to interpolate between the 6 h data points with sufficient accuracy (Li et al., 2015). The new Figures 9 and 16 showing time series of hydrostatic gradients from ECMWF also confirm the low variability during time periods of 6 h.
Section 4.2 was split into two parts. (We agree that these were two rather different topics).
We did not split Section 5.1. It has changed significantly with the testing of several different GPS solutions.
Specific comments

P1L11: 15-day long continuous
Corrected

P2L4: VLBI, GPS and WVR (remove closing bracket).
Corrected

P2L12: a 4-year period
Corrected

P2L13: a 15-day long VLBI campaign
Corrected

P2L20: over long-time scales
We are not sure about this. "long" is an adjective and "time scales" are two nouns. After talking to a native English speaker we decide to keep it as it is.
No change in the manuscript.

P6Tab2: add gradient mapping function and reference frame and PCV values applied (IGS08 or IGS14?)
The Bar-Sever et al. (1998) the mapping function was used for the gradient estimation. The reference frame is IGS08. Table 2 describing the GPS data processing has been updated with this information.

P6L6: (consider modified wording) ... estimated gradients are independent in adjacent epochs ...
Instead we write: "estimated gradients are independent of the ones estimated at adjacent epochs ..."

P9L15: ... as piece-wise linear offsets ... Do you mean representation with a piecewise linear function when represented with the interval end-point offsets? Or do you mean just constant offsets for individual intervals? Please, reword or clarify.
We changed the wording to "piecewise linear continuous function"
This is also illustrated in the new Figures 14 and 17, but of course the reader may not yet have seen these figures while reading this section.

P11L5: the overall mean negative north gradients is also partly attributed to the flattening of the earth atmosphere, see Meindl et al. 2004, I suggest to add in the discussion in this paragraph.
We do not find any statement in Meindl (2004) about the flattening of the earth atmosphere. We also find that Meindl (2004) only refer to the negative north gradients as a function of latitude. Therefore, we removed the word "pressure" from our text in order to give a correct citation.

P12 Figure 9: discuss the different ranges of gradient sizes,
Gradient sizes are now discussed together with the new Figure 11.

P13L6: by long-term averaging ...
Corrected

P13L18: ... at this low humidity level ...
Corrected

P13L19: I suggest to add here new sub-sections for discussing long-term trends in gradients. I found it confusing when mixed in a single section.
Done

P13L21: a possibility ...
Corrected

P13L22: trends in the total amplitude value of the gradients (I don't understand what is meant exactly by the trend in the total amplitude value of gradients. It would be helpful to clarify it here)
The total amplitude is > 0. If the variability increases along one coordinate there will be larger gradients, both positive and negative. This can happen without a net increase (trend) in the east and north gradient component.
This text is rewritten and the mathematical definition of "total amplitude" is added.

P13L22: A positive trend in the amplitude will occur if there is an increase in the variability at the side which can happen even if there are no trend ... (confused again how to understand the meaning of the sentence).
See previous comment.

P15Sec5: Consider modifying Sect 5.1 title by adding WVR so it is easier to distinguish which paragraphs compare GPS to WVR, and GPS to VLBI (5.2). Optionally, split 5.1 into sub-sections dealing with original and averaged comparisons.
Titles are modified — additionally now also WVR data are compared in Section 5.2.

P15L5: ... sites share several error sources ... (suggest to specify them more)
We now mention satellite clock and orbit errors and mapping functions.

P16Fig11: I suggest also discussing more ranges of estimated gradients, which seem different for GPS and WVR. GPS gradients are generally smaller. E.g. it could be due to constraining in GPS solution, mapping function, elevation angle cut-off, elevation dependent weighting or other effects. Similarly, it seems for GPS vs VLBI, where VLBI gradients seem to be more smoothed than GPS, most likely due to the 6-hour temporal resolution.
We think the amplitudes of the GPS and WVR gradients are now also addressed by the new Figure 11. Concerning the VLBI gradients we think it is difficult to make a general statement about their amplitude size. However, given that the sampling of the atmosphere is much more sparse, a short lived gradient in combination with assumption of linear functions in 6-hour segments, will probably reduce the variability in the estimated amplitude. We added this comment when discussing the new Figure 15.

P16L7: wet gradients from both GPS stations, ONSA and ONS1, ... (suggesting for a better clarity)
Corrected

P17Fig12: it seems that giving correlation coefficients in the text is enough, without further need to show both plots which characteristics are the same as in Figure 11.
We agree and remove the figure but keep the text.

P18Fig13: Consider merging four plots into a single one with the x-axis ranging in 2013 to 2016

We did consider this, but think that it is easier to identify the specific month and compare it between the different years. We keep it as it is.

P22L6: we find the wet component of the gradients cause most of the variability. (removed 'to')

Corrected

P22L15: if small gradient trends ... (remove plural)

Corrected

Referee #3:

There was a time when tropospheric delays were considered as error-prone parameters that had to be corrected by meteorological observations from other instruments. Successive methodological improvements have led Zenithal Wet Delay retrieved by GNSS to be sufficiently accurate for use in meteorology and climatology. The information content in linear horizontal delay gradients estimated from space geodesy observations is the next step, the central issue that must be treated rigorously so as not to lead to misinterpretations or over interpretations whose consequences can be unfortunate for the applications that come out of them. At first sight, the article is presented as providing general answers to this problem.
However, the results obtained are valid only in Sweden, in a particular meteorological context (the Icelandic low pressure system), in a particular geodesic context (the poorer sampling of GPS data on the sky north of the zenith direction due to the geometry of the GPS satellite constellation which is particularly the problem at high latitude) and mainly using the statistical notion of correlation coefficient. These results deserve to be verified on a global scale even if this study is an interesting intermediate step.
However, the title should reflect the true scope of this study.
We do not agree that all results are only valid in Sweden. The meteorological processes mentioned, such as changes of air masses and systematic patterns in the pressure, are frequent in many regions. Also the possible instrumental effects related to anti reflecting material at the antenna is a general result. Since we clearly state in the abstract that we only use 5 sites in Sweden we want the title unchanged. Although we are not native English speakers it is our interpretation that the first two words of title indicate that it is a modest contribution to a complex subject.

Moreover it would have been interesting to provide more bibliographic references to list the results previously obtained for other regions and to compare them with the results of this study.
This study deals with the concept of total, hydrostatic or wet gradients, of pressure gradient, of temperature gradient, of water vapor gradient, of wet gradient retrieved by WVR. However, these notions are not sufficiently defined or sufficiently documented by bibliographic elements, which undermines the clarity of the article. The reproducibility of the results of this article should be facilitated: -> Where can we download GPS, WVR and ECMWF data? -> How to estimate the gradients with the WVR? -> What are the options used to process the data in detail? If there are studies, technical reports or more general articles that can provide quick and accurate answers to these questions without lengthening the article excessively: perfect, if not the addition of elements in the supplemental material could be a good option.
It would have been necessary to give some elements on the comparisons between ZWD estimated by the different techniques before deepening the comparison of the gradients.
We believe that we have addressed all these points in the revised manuscript. They overlap with several of the specific points from all three referees. We will come back to these in the specific comments below.

One of the listed points of the summary is the comparison of the GPS gradients with the corresponding ones from the ECMW analyses. How GPS gradients can confirm known seasonal effects both in the hydrostatic and the wet components whereas GPS gradients are total gradients exclusively? In fact, it is an assumption that ECMWF hydrostatic gradients are reasonably accurate (P13L13). Before subtracting the ECMWF hydrostatic gradients from the total GPS gradients, rigorously, it would have been necessary to ensure that the hydrostatic gradients calculated by the ECMWF and felt by the GPS measurements are equivalent, which seems very difficult to verify.
We do say that it is an assumption. In order to a give a bit more motivation, showing that it is a reasonable assumption, in the revised manuscript we have two new Figures (9 and 16) that show the

different behaviour both in amplitude and in temporal variability of the wet and hydrostatic gradients from ECMWF.
The assumption is also motivated by that when WVR gradients are correlated with GPS gradients the correlation increases when the hydrostatic gradient from ECMWF is removed from the GPS total gradients. This improvement in correlation coefficients is now explicitly given in the caption to the new Figure 13.

The main statistical comparison tool is based on the notion of linear correlation. However, the article does not explain the advantages, disadvantages and limitations of this approach without any specific bibliography for this type of study. Again, it undermines the clarity of the article and the scope of its conclusions.
We have added standard deviations (SD) and state that correlation coefficients also are presented motivated by the different gradient amplitudes. They are used in a relative sense if an agreement is better or worse given identical input data but processed differently. Although we note that the comparison of the agreement between WVR and different GPS solution give the same result using SD as using correlation coefficients.

With just 13 lines in the article,
the results of the CONT14 VLBI measurement campaign seem insufficiently exploited.
The sampling of the sky is a critical parameter according to the authors, what are the further studies to be conducted to avoid or reduce this problem?
We have now added WVR gradients and make additional comparisons (see the overall changes at the beginning of the document).
We have added a short paragraph about the future of geodetic VLBI with the VGOS system.

Taking into account the preceding remarks and clarifying the points raised, the article could then serve as a reference for future studies.

Here are my specific comments.

P1L1 : " . We assess the quality of estimated linear horizontal gradients in the atmospheric propagation delay " versus
The "versus" comes in the 3rd sentence of the abstract which should be fine, or did we not understand?

P1L21 : " the reproducibility of estimated geodetic parameters " improper term ? / Repeatability?
According to e.g. NIST https://www.nist.gov/pml/nist-tn-1297-appendix-d-clarification-and-additional-guidance, the so called repeatability conditions are:
- the same measurement procedure
- the same observer
- the same measuring instrument, used under the same conditions
- the same location
- repetition over a short period of time

We think that for long time series of geodetic parameters, the term reproducibility should be used.

P2 : Figure 1 is a very rough picture of the real situation. Orders of magnitude are given without any explanation. Is the Earth modeled as an infinite plane or sphericity is taken into account? " The scale heights, hs of the hydrostatic refractivity and the wet refractivity are approximately 8 km and 2 km, respectively. " 8 km / 2 km ... Proof? References?

With the added theoretical background we can now refer to Equation (2) for the refractivities and we pointed out that there are large variations as well as that the sampling of the volume can and will be different for different instruments. The text of the figure is rewritten saying that it is a sketch, that the scale heights vary a lot, and referring to Eq. (2). We think every reader knows that the mapping functions used later in the modelling takes the sphericity of the earth into account, or ...?

P2L4-6 : " Gradinarsky et al. (2000) found that using different constraints for the variability of the horizontal gradient in the VLBI and GPS data analysis did not have a significant impact on the agreement with the WVR estimates. " Can you be more explicit and provide quantitative data?
The above sentence is replaced by:
Gradinarsky et al. (2000) found that when varying the constraint for the gradient variability from 0.2 to 5.6 mm/\sqrt{\rm h} the weighted root-mean-square (rms) difference compared to the WVR gradients varied between 0.8 and 1.0 mm for both the GPS and the VLBI gradients.

P2L6-7 : " A more recent study by Li et al. (2015) reported on the improvement obtained by Using multi-GNSS constellations instead of GPS only. " Can you explicit with quantitative results?
The following text replaces the one above in the revised paper "Using multi-GNSS observations, Li et al. (2015) found a significant increase in the correlation coefficient to about 0.6 when compared to ECMWF gradients, while the one for the GPS only was typically below 0.5. In addition, they found that the RMS difference of the gradient is reduced to about 25–35 % by multi-GNSS processing."

P2L16-17 : OK it is known but provide the major references ...
A reference to Rüeger (2002) is added together with the equation for refractivity and additional references follow in the same section.

P2L18: " Hydrostatic gradients " These terms are not defined in the article and are not commonly used.
These are now defined in the theoretical background in the beginning of Section 2.

P2L18-20: unclear
See the response above.

P2L20: see IERS conventions (2010)
We added also this reference in the theoretical background text describing the model.

P3L1: Provide more recent references. What are the scientific questions raised by this climatic specificity?
It is a well known meteorological feature (that affects space geodesy data). It is a confirmation that the gradients estimated from space geodesy data are correct (in this sense).
Two additional references are added.

P3L3: "Temperature and especially water vapour can show relatively much stronger horizontal gradients over small (kilometre) scales. The temporal variability is typically also much higher than that of the hydrostatic gradients, see e.g. Li et al. (2015). ": equations? References? Which temperature? Ground? Column? How are obtained these order of magnitude? [Typo : kilometer]
Equations have been added in Section 2.
We have also added the two new Figures 9 and 16, showing time series of hydrostatic and wet gradients from the ECMWF data.
We use British English and according to our dictionary the spelling is "kilometre"

P3L6 : " be significant during a passage of a weather front, especially for distinct cold fronts." order of magnitude

With the extension of Section 5.2 in the revised manuscript gradients associated with the change of air masses are shown. This is however, not very helpful here in the introductory part. Since we did not find a reference of gradients estimated during the passage of a "distinct cold front". We changed the text and referred to Kacmarik et al. (2018) and their estimated gradients during an occlusion front.

P3L7-8: Provide references that study these phenomenons with GNSS data.

We are not aware of published results that identify estimated GNSS gradients with a specific source, except for the fronts mentioned above. The following examples mention meteorological phenomena that have horizontal variability in the partial pressure of water vapour and with the equations now included in the beginning of Section 2, this should be clear. The text is rephrased and now first mention variability in the partial pressure of water vapour.

P3L16-17: software and references ...
Table 2 is expanded and updated

P4L3 : Ning et al (2013) : It would be interesting to speak about an eventual update of the procedure ... atx file should have been updated for instance ...

The atx file has been updated. This is specified in Table 2, including a footnote for the reprocessing done for the 4 years of data from the Onsala site for the revised version of the manuscript.

P4L4 : " we calculated mean values over 15 min, 1 h, 6 h, 1 day, and 1 month. " Ok but why? Specify scientific questions in term of atmospheric processes
Examples of atmospheric processes that affect the 3D refractivity over time were mentioned in the previous section. The 1 h was a mistake. The new text is:
" we calculated mean values over 15 min, 6 h, 1 day, and 1 month
in order to match the temporal resolution of the comparison data
and to study the variability of the wet and the hydrostatic gradients over different time scales."

P4L5-7: Figure 4 shows Figure 1 is too simplistic. May be presenting the problem like this?
We now point out the issue of sampling already in the caption to Figure 1.

P4L9-11 : references or technical report to provide ? What are the problems of this technique? Advantage and limitations?
A general reference to Elgered and Jarlemark (1998) is added. In the caption to Figure 6 we now mention that observations cannot be done in directions close to the sun and not below elevation angles of 20°.

P6L1-2 : " Therefore, data taken during rain, or when the estimated amount of liquid water is >0.7 mm, are discarded from the analysis. " references ? If we do not pay attention: what are the consequences? Bias? Ok for rain but without rain : precision ?
A reference to Westwater and Guiraud (1980) is added and we especially mention "large positive errors in the wet delay".

P6L2-3 " when the WVR hardware has failed. " Why?
We added brief information for to 2 long data gaps:
The first long data gap in 2014–2015 was caused by a broken mechanical waveguide switch
and the second long gap in 2015–2016 was due to broken cables in the so called cable wrap. The cable wrap was redesigned.

P7L21-2: → It would be interesting to provide a reference which explains the observations

and the estimation of SWD with this instrument. It would be interesting to explain how the WVR gradients have been computed. → " where constraints with time are applied. " Specifically with your solution with GIPSY. → It would be interesting to recall what is observed and what is modeled with GNSS and WVR. Or provide references ...
The GNSS gradients were estimated using a random walk model with a standard deviation (SD) of 0.3 mm/sqrt(h)) that was taken from Bar-Sever et al. (1998). A reference to Jarlemark et al. (1998) is added in Table 2 for the GPS constraint for the ZWD.
The reference to Elgered and Jarlemark (1998) above and references therein explains the SWD/ZWD calculation with the WVR. We state that the WVR gradients use the "four-parameter model" in Davis et al. (1993).

P8 Figure 7: → optionally add rainfall? → Difference between [2013,2016] and [2016,2017] about the maximum number of daily data : around 10000 / > 10000 / Homogenous methodology of WVR observation ? → Histogram?
We think it would be too detailed to add rainfall information (since it occurs often and is the major cause for data loss except for the 2 long gaps). We now note that in the text and stress that the same observation sequence is used over the 4-year period as well as mention that observations close to the sun are removed (in the caption to Figure 7).

P9L15-17 : Are you sure of the units about the constraints ?
Yes, we now also note that they are not modelled as stochastic processes.

P9L16-17 : inhomogeneity between mapping functions ...
In the revised paper, we also processed the GPS data using the same mapping function (NMF) and found that NMF or VMF1 did not have a large impact on the gradient correlation with the WVR.

P9 part 3.4 : Focus on scientific and methodological questions ? Not enough details are given : impossible to reproduce the study.
Details have been added both on the motivation for the CONT campaigns and missing information about gradient mapping function and elevation cutoff angle.

P11L3 : Figure 9 : why do not use monthly running average ?
We could have done that but chose to illustrate the 11 years of data for each month to visualize any seasonal variation.

P11L4 : 10° or 20° ? What are the differences of the two GPS solutions? Which one is chosen? Why ?
In the revised paper, we added more results on the gradients given by different GPS solutions, i.e., different elevation cutoff angles, weighting and non-weighting, different mapping functions. We used the gradients given by the GPS 3° cutoff angle solution for all other comparison due to a better agreement when compared to WVR gradients.

P11L5 : " We can clearly see negative north gradient in the winter both in the GPS and the ECMWF results. " provide quantitative results
We added -0.2 mm as a mean value.

P11L7 : " the Icelandic low pressure system (Hewson and Longley, 1944). " Only one reference ... 1944 ...
Two more recent references were added in Section 2. Here we refer back to this.

P11L9-12 : add references / Why WVR data have not been used ?
Two additional sea breeze references were added in Section 2. Unfortunately, WVR data from scanning the sky are not available for the 11-year period only for 2013-2016. We say that sea breeze is

one possible cause, we do not claim that this is what we see. Perhaps in a future collaboration with meteorological expertise we could study sea breeze conditions using both GNSS and the WVR.

P13 Table 4 : 6-hour resolution of ECMWF data It seems difficult to draw conclusions from hourly comparison between GPS and ECMWF.
This was a mistake — thank you for making us aware of it. It is corrected to "six hourly".

P13L2-3 : " We assess the data quality, in terms of correlation coefficients, between the total GPS and ECMWF gradients estimated at the 5 GPS sites using data from 2006 to 2016. These are shown in Table 4. " The linear correlation coefficient is mainly used in this study: what are the advantages and disadvantages of the methodology followed?
Correlation coefficients are used in a relative sense by comparing the agreement at different stations. In Section 5 where we also use WVR data (that in general result in larger gradient amplitudes) we also use standard deviation to compare the agreements. The results are consistent.

P13L10-12 : " . 10 Another result worth noting is that the two sites with the highest correlation coefficients, and especially for the monthly averages, are ONSA and SPT0. These two sites are the only ones that are equipped with microwave absorbing material below the antenna. This could reduce the impact from unwanted multipath effects. The phenomenon calls for further studies. " It would be divergent with page 17 line 10 : "Comparing the results obtained for ONSA with those from ONS1 they are almost identical (in both Figures 11 and 13) meaning that in this case there is no obvious improvement from the absorbing material below the antenna on ONSA."
We give a possible explanation for this: "Our assumption is that the lack of a concrete pillar with a metal mounting plate just below the antenna on ONS1 eliminates the need for an absorber"

P13L13-15 : " Assuming that the ECMWF hydrostatic gradients, linearly interpolated between the 6 h values, are reasonably accurate we have the possibility to subtract this hydrostatic gradient from the estimated total GPS gradient in order to compare the wet gradients at these five sites " Provide a reference to justify the approach
See above — actually there was no interpolation. It is the "six hourly" values that are compared. We now refer to this comparison to be "six hourly"? This is done in both Table 4 and Table 5.

P13L16 : " We note that when the wet gradients are averaged over one hour and one day " Did you subtract the daily average before calculating the hourly average?
The 6 hour averages are the averages of the gradients over the 6 h. No daily average was subtracted. As mentioned above, hourly is changed to 6 h.

P14L3 " Typically they are all well below 0.01 mm/year. " Have you tested the significance?
No we did not, but we should have done that. Now we have calculated two different formal uncertainties and expanded the text. It is clear (we think) that no atmospheric gradient trend has been detected, but we still mention the highest trend estimated, and warn for instrumental effects when searching for trends in the future.

P15L5 " We expect that the two GPS sites share several error sources " OK, more detail should be given about GPS errors
We now mention satellite clock and orbit errors when observing the same satellites and we use the same mapping function (same as Referee #2)

P15L6 " there is a significant common mode suppression of errors " GPS data have been processed by PPP ... Can you explain more what you mean by "a significant common mode suppression of errors"? Do you speak about the common modelling to

process GPS data?
Yes, a common modelling and common errors associated with the same observed satellites (see the previous comment).

P15L6 : " be slightly overoptimistic. " that needs more investigation
We removed "slightly". It is just overoptimistic, because of the shared common errors mentioned above, but we cannot quantify how much.

P15 Figure 10 : There are differences that seem to be systematic over short periods of time ... (presence of dotted curves in this figure unlike Figure 11)
In the new Figure 12, we plot the GPS gradients with the original temporal resolution of 5 min. When compared to WVR data, in Figure 13 (middle and right), the GPS gradients were averaged to a 15 min temporal resolution in order to match the WVR data. We now state this in the figure captions.

P15L17-18 : Amplitude of the North component versus amplitude of the East component?
We did several plots of east versus north gradients and found that they were not correlated at all, so we did not pursue this further.

P15L4 " reduced at the order of 10 % " 10° to 20° reduces the correlation coefficients ... What happens if you reduce the cutoff from 10° to 5° or below ?
The question is dealt with in the new GPS solutions using cutoff angles of 3°, 10°, and 20°. Section 5.1 is significantly expanded with these new results.

P17L2-3 "). The other reason is the much higher variability in the time series from the WVR because no temporal constraints are used when estimating these gradients. " References about WVR and how its gradients have been estimated are necessary for a better understanding. Is it possible to add a stochastic constraint to estimate WVR gradients? I do not know if you can change the procedure to estimate tropospheric delays by WVR.
The description of the WVR and the estimated gradients is updated in Section 3. In principle, there is nothing that would not allow constraints to be applied in the WVR gradient estimation. However, that is a big effort (at least for us). We choose to discuss this as possible future work in the Conclusions section.

P17L6 : typo : Lu et al. (2016) Figure 8 of Lu et al. (2016)
Corrected

P17L10 " there is no obvious improvement from the absorbing material below the antenna on ONSA." the cutoff angle is fixed at 10° ... The effect of the absorbing material would be shown using a lower cutoff angle.
We processed the ONSA data using a 3° elevation cutoff angle and the result is the same, still there is no clear difference between ONSA and ONS1.

P12-13 " ECMWF gradients compared to the KIR0, MAR6, and VIS0 sites. Our assumption is that the lack of a concrete pillar with a metal mounting plate just below the antenna on ONS1 eliminates the need for an absorber (see Figure 3). " Good hypothesis that deserves to be confirmed: references on IGS network ?
Sorry, we have not been able to find any independent confirmation, someone has to be first ... However, to be fair, when the Swedish Mapping, Cadastral and Land Registration Authority designed the monument for ONS1 it was suspected that the original design of monuments in the SWEPOS reference network was not optimal.

P18 Figure 13 : The norm of monthly wet gradient as a bar plot would be interesting.

In the original manuscript we did not have any time series plot in Section 5.1. This comment, plus a few other comments, addresses the issue of the different gradient amplitudes. The new Figure 11 address these issues. Here the absolute value of the monthly means of the wet gradients are shown together with the ZWD monthly means from ONSA, ONS1, and the WVR. The idea is that these qualitative graphs show correlations that are clear to the eye offer a better understanding compared to additional correlation plots.

P19 part 5.2 : This part is a little disconnected from others and is not thorough enough to allow a clearer view of the contribution of VLBI to this study. More questions about the representativity of the gradients estimated by the geodetic techniques are araised. We would expect more answers on this issue.
When we added the WVR data for comparisons during this 15-day period we find that the temporal resolution of 6 h is limiting the study. The main result, we think, that is discussed in the updated text, is that we can try to motivate additional gradient studies using the upcoming VGOS.

P19 L6-7 : " We note that the agreement in general is better for the east component compared to the north " amplitudes of East and North Component ?
Better language: "Again we note that the agreement, in terms of correlation coefficients, is better for the east component compared to the north component."

P19L7-8 : " where a large north gradient is not detected in the VLBI data. " How are estimated the VLBI gradients? Stochastic constraints? Impact of the 6 hour resolution? How gradients are modeled in the VLBI data processing? Step? Piecewise linear function?
The text in Section 3 has been updated to describe that the gradients are estimated as piecewise linear continuous functions and not a stochastic process.

P21 Figure 15 : " and the black dots are linearly interpolated VLBI results with a temporal resolution of 5 min in order to match the GPS data. " The interpolation must be consistent with the gradient modeling used for VLBI data processing. Can you clarify?
The figure has been removed from the manuscript. Instead a table with correlation coefficients for VLBI-GPS and VLBI-WVR has been added.

P21 Figure 15:" using mean values for the period of ±3 h around the time epochs of the VLBI values (6h:) " same remark as before: The 6-hour resampling of GPS estimates must be consistent with the gradient modeling used for VLBI data processing. Here, that implies that VLBI estimates are modeled as a step function.
Since the figure is removed it does not matter. (However, it can be consistent if also the continuous VLBI segments are averaged around the given value ± 3 h.)

P22L6-7: " When studying gradients averaged over shorter time scales, e.g. 15 min, we find the wet component of the gradients to cause most of the variability " Not exactly because you subtracted the hydrostatic gradients sampled at 6 h from the ECMWF. You did not analyze the variability of the hydrostatic gradients.
We have now added a plot (Figure 16) with ECMWF hydrostatic and wet gradients in Section 5.2. It is not 100 % safe but looking at the change from one 6-hour value to the next indicates that not much is happening in between.

P22L10: "during the warmer, and more humid, part of the year " It would have been interesting to use IWV retrieved by GPS.
The new Figure 11 addresses this issue. (ZWD is roughly proportional to the IWV.)

P22L11-12 " s in the east compared to the north direction. " It would have been interesting

to better cross the amplitude of the gradients with the correlation coefficients obtained.
We do not understand what is meant, unless it is covered by the new Figure 11 in combination with the old figure with the new number 14? No other action has been taken related to this comment.

P22L12-14 " We interpret this difference to be caused by an inhomogeneous spatial sampling on the sky, which is important when we assume that the model describing linear horizontal gradients has deficiencies. The different sampling on the sky is an important issue for any comparison between different techniques. " This question remains unresolved and would have to be studied later.
Yes, that is what we meant. We have added the suggested sentence.

P22: Lack of " Data availability section"
We now give the IP addresses for the input data. The gradient time series estimated by us using GPS, VLBI, and WVR data have been archived and approved in terms of the documentation by the Swedish National Data Service (SND) and a doi number will be sent to us within days, so that it can be published in the final version. For the time being a compressed file is available via DropBox: https://www.dropbox.com/s/lg4sctpm6qrfto4/Gradient%20data.zip?dl=0

On the information content in linear horizontal delay gradients estimated from space geodesy observations

Gunnar Elgered[1], Tong Ning[2], Peter Forkman[1], and Rüdiger Haas[1]

[1]Department of Space, Earth and Environment, Chalmers University of Technology, Onsala Space Observatory, SE-43992 Onsala, Sweden.

[2]Lantmäteriet (The Swedish Mapping, Cadastral and Land Registration Authority), SE-80182, Gävle, Sweden

Correspondence: Gunnar Elgered (gunnar.elgered@chalmers.se)

Abstract. We assess the quality of estimated linear horizontal gradients in the atmospheric propagation delay above ground-based stations receiving signals from the Global Positioning System (GPS). Gradients are estimated from 11 years of observations from five ~~sites~~ stations in Sweden. Comparing these gradients with the corresponding ones from the European Centre for Medium-Range Weather Forecasts (ECMWF) analyses show that GPS gradients confirm known seasonal effects both in the hydrostatic and the wet components. The two GPS ~~sites~~ stations equipped with microwave absorbing material below the antenna in general show higher correlation coefficients with the ECMWF gradients compared to the other three ~~sites~~stations. We also estimated gradients using GPS data from two collocated antenna installations at the Onsala Space Observatory. Correlation coefficients for the east and the north wet gradients from GPS can for specific months reach up to 0.8 when compared to simultaneously estimated wet gradients from microwave radiometry. The best agreement is obtained when an elevation cutoff angle of 3° is applied in the GPS data processing, in spite of the fact that the radiometer does not observe below 20°. Based on the four years of results we note a strong seasonal dependence in the correlation coefficients, from 0.3 during months with smaller gradients to 0.8 during months with larger gradients, typically during the warmer, and more humid, part of the year. Finally, a case study using a ~~15 days~~ 15-day long continuous Very Long Baseline Interferometry (VLBI) campaign was carried out. The comparison of the gradients estimated from VLBI and GPS data indicates that a homogeneous and frequent sampling of the sky is a critical parameter.

1 Introduction

Space geodetic techniques, where the fundamental observable is a radio signal's time of arrival at a ~~site~~ station on the surface of the Earth, are affected by variations in the propagation velocity in the atmosphere. Because time measurements avoid problems related to accurate calibration, which are common for systems measuring different types of emissions, it is a common view that Global Navigation Satellite Systems (GNSS) have a long term stability and are well suited for climate monitoring, e.g. in terms of the atmospheric water vapour content. Estimates of the total propagation delay above a GNSS ~~site~~ station can be used to determine the integrated amount of water vapour. It is also common practice to estimate two-dimensional horizontal linear gradients for each ~~site~~ station in the GNSS data processing, because it improves the reproducibility of estimated geodetic parameters, see e.g. (Bar-Sever et al., 1998).

We ~~address the question of the~~ assess the quality of the estimated gradients primarily from GPS data from Swedish GNSS ~~sites~~ stations by comparing these gradients to independent measurements. An important site is the ~~fundamental geodetic station at the~~ Onsala Space Observatory where a geodetic Very Long Baseline Interferometry (VLBI) telescope and a water vapour radiometer (WVR) are installed collocated to GNSS receiver stations. The overall goal ~~is to thereby~~ of this study is to assess the usefulness of GPS-derived gradients in atmospheric and climate research. Previous studies have been carried out using GPS/GNSS data from Onsala. Comparing the horizontal gradients derived from VLBI~~)~~, GPS, and a WVR, Gradinarsky et al. (2000) found that ~~using different constraints for the variability of the horizontal gradient in the VLBI and GPS data analysis did not have a significant impact on the agreement with the WVR estimates. A more recent study by Li et al. (2015) reported on the improvement obtained by using~~ when varying the constraint for the gradient variability from 0.2 to 5.6 mm/$\sqrt{\text{h}}$ the weighted root-mean-square (rms) difference compared to the WVR gradients varied between 0.8 and 1.0 mm for both the GPS and the VLBI gradients. Using multi-GNSS ~~constellations instead of GPS only~~observations, Li et al. (2015) found a significant increase in the correlation coefficient to about 0.6 when compared to ECMWF gradients, while the one for the GPS only was typically below 0.5. In addition, they found that the RMS difference of the gradient is reduced to about 25–35 % by multi-GNSS processing.

In Section 2 we give a short background on the cause of horizontal gradients that are sensed by the space geodetic techniques and the model used to estimate them. In Section 3 instruments, techniques, and their data are described. The results are presented in two sections. First, in Section 4, we use 11 years of data to study the gradients from five Swedish GNSS ~~sites~~ stations and assess their quality by comparing them to gradients originating from the European Centre for Medium-Range Weather Forecasts (ECMWF) analyses. In Section 5, we use data from two collocated GNSS ~~sites~~ stations and one WVR to assess the accuracy of the gradients during a ~~four year~~ 4-year period. Within this period we also carry out a comparison to gradients estimated from a ~~15 day~~ 15-day long VLBI campaign. Finally, in Section 6 we present our conclusions and discuss possible future studies of gradients.

2 Cause of horizontal gradients and models

The ~~refractivity in the atmosphere~~ delay of space geodetic signals propagating through the atmosphere depends of the refractive index n. Because the values are typically just above 1 it is practical to define the refractivity, $N = 10^6 (n-1)$. A common expression used for the refractivity is (Rüeger, 2002)

$$N = k_1 \frac{p_d}{T} + k_2 \frac{e}{T} + k_3 \frac{e}{T^2} \tag{1}$$

where p_d is ~~determined mainly by the total pressure,~~ the ~~temperature and the~~ partial pressure of ~~water vapour. The atmospheric volume sensed by a GNSS instrument~~ the dry constituents of air in hPa, e is the partial pressure of water vapour in hPa (i.e., the total pressure $P = p_d + e$), and T is the absolute temperature in K. The values of k_1, k_2, and k_3 are estimated from laboratory

experiments. For space geodetic applications it is meaningful to combine the terms resulting in two refractivity components, often referred to the hydrostatic (N_h) and the wet (N_w) components (Davis et al., 1985):

$$N = N_h + N_w = k_1 \frac{P}{T} + k_3' \frac{e}{T^2} \tag{2}$$

In order to define the integrated horizontal delay gradient, that can be inferred from ground-based observations, we follow Davis et al. (1993) and start by expressing the refractivity as a function of the height z, the horizontal vector $\boldsymbol{x}$, consisting of one east and one north component, and the time t:

$$N(\boldsymbol{x}, z; t) = N_\circ(z; t) + \boldsymbol{\xi}(z; t) \cdot \boldsymbol{x} \tag{3}$$

where $N_\circ(z; t)$ is the vertical profile of the refractivity at $\boldsymbol{x} = 0$ and $\boldsymbol{\xi}(z; t)$ is the vertical profile of the horizontal gradient at $\boldsymbol{x} = 0$:

$$\xi_i(z; t) = \left. \frac{\partial N(\boldsymbol{x}, z; t)}{\partial x_i} \right|_{\boldsymbol{x}=0} \tag{4}$$

where the index $i = 1, 2$ denotes the east and the north direction, respectively. This leads to the following expression for the integrated horizontal delay gradient:

$$\boldsymbol{\Xi} = 10^{-6} \int_0^\infty dz \; z \; \boldsymbol{\xi}(z) \tag{5}$$

Hence, the vector $\boldsymbol{\Xi}$ has one east and one north component, which in turn can be separated into one hydrostatic and one wet component according to Eq. (2). The atmospheric volume that is more or less homogeneously sampled by ground-based sensors such as a GNSS station, a VLBI station, or a WVR, is illustrated in Figure 1.

Hydrostatic gradients are usually dominated by pressure gradients and exist mainly over global and regional scales (e.g. ~~mesoscale~~ synoptic scale weather systems). For example the north gradient has a clear dependence ~~of pressure and~~ on latitude when averaged over long time scales. This has been shown by Meindl et al. (2004) using GPS data. For the area of interest in this study we specifically mention the Icelandic low pressure system that typically evolves in the winter and disappears in the summer, e.g. ~~(Hewson and Longley, 1944)~~(Hewson and Longley, 1944; Thompson and Wallace, 1998; Sanchez-Franks et al., 2016).

Temperature and especially water vapour can show ~~relatively much stronger~~ strong horizontal gradients over small (kilometre) scales ~~. The~~ and the temporal variability is typically also much higher than that of the hydrostatic gradients, see e.g. Li et al. (2015). Hence, the large local gradients over a ~~site~~ station are mainly caused by the variability in water vapour and the wet refractivity. Gradients can be significant during a passage of a weather front, ~~especially for distinct cold fronts.~~e.g.

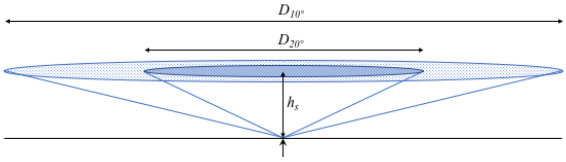

Figure 1. ~~The~~ A sketch showing that the atmospheric volume determining the estimated atmospheric parameters is a cone originating at the upward pointing arrow. The typical scale heights, h_s of the hydrostatic refractivity and the wet refractivity are ~~approximately~~ of the order of 8 km and 2 km, respectively, but vary a lot globally and in time according to Eq. (2). For the hydrostatic refractivity the diameter of the cone at the scale height is 91 km ($D_{10°}$) and 44 km ($D_{20°}$) for the elevation cutoff angles equal to 10° and 20°, respectively. The corresponding diameters for the cones representing the wet refractivity are 23 km and 11 km, respectively. Note that the horizontal and vertical scales are different.

Kačmařík et al. (2018) report gradient amplitudes of up to 3–4 mm during the passage of an occlusion front over Germany. Other specific weather phenomena that can cause horizontal variability in the partial pressure of water vapour, and hence also the wet refractivity, are sea breeze ~~(?)~~(Craig et al., 1945; Miller et al., 2003), cloud rolls (Brown, 1970) and convection processes in general. We note that none of the known processes is expected to be strictly linear, but the strength in the geometry and the GNSS data quality have so far not motivated ~~attempts~~ to determine additional atmospheric parameters of higher order.

The atmospheric parameters that are normally estimated when processing space geodesy data are an equivalent zenith wet delay and linear horizontal delay gradients in the east and the north directions. The uncertainties of the estimates depend on the geometry of the observations and the accuracy of the so called mapping functions, used to describe the estimated parameters dependence on the elevation angle, given the specific weather conditions at the site, at the time, see e.g. Boehm et al. (2006) and Kačmařík et al. (2018). The common model used to relate the observed delay along the line-of-sight, $\Delta L(\alpha,\varepsilon)$, and the estimated parameters (IERS Conventions, 2010) is also used in this study, i.e.

$$\Delta L(\alpha,\varepsilon) = m_h(\varepsilon)\,\Delta L_{hz} + m_w(\varepsilon)\,\Delta L_{wz} + m_g(\varepsilon)\,[\Xi_e \sin\alpha + \Xi_n \cos\alpha] \tag{6}$$

where m_h, m_w, and m_g are the mapping functions, depending on the elevation angle ε, for the hydrostatic and wet delays, and the horizontal gradients, respectively; ΔL_{hz} and ΔL_{wz} are the equivalent hydrostatic and wet delays in the zenith direction; α is the azimuth angle, measured clockwise from the north, implying that Ξ_e and Ξ_n are the horizontal delay gradients in the east and in the north directions.

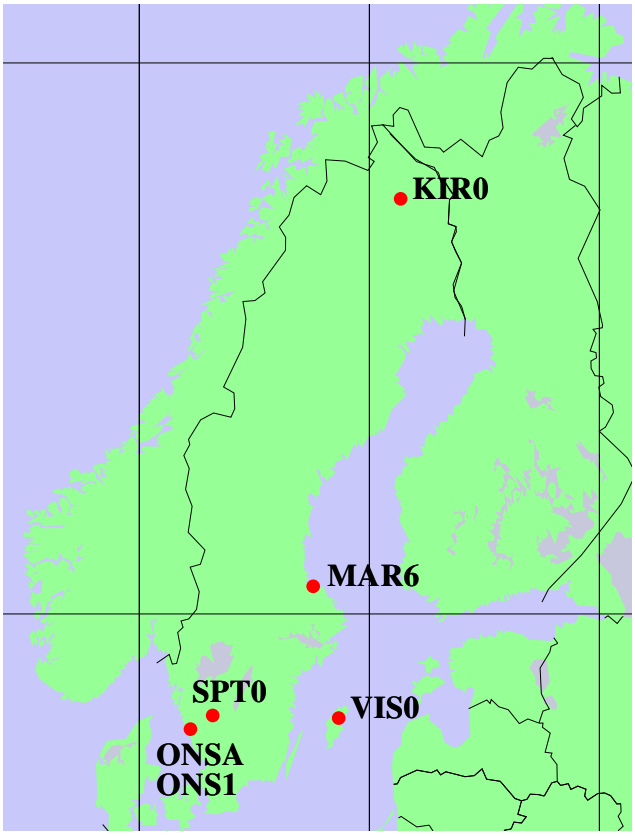

Figure 2. The six GPS ~~sites~~ stations used in the study. ONSA and ONS1 are collocated together with the VLBI telescope and the WVR at the Onsala Space Observatory.

3 Instrumentation and data

We compare horizontal gradients estimated from GPS observations acquired at five sites and six antenna/receiver installations: Kiruna (KIR0), Mårtsbo (MAR6), Onsala (ONSA and ONS1), Borås (SPT0), and Visby (VIS0)~~. These sites~~, with respect to VLBI, WVR, and ECMWF estimates. These stations are also part of the EUREF network (Bruyninx et al., 2012). Their geographic locations are shown in Figure 2 and the used datasets are summarised in Table 1.

3.1 GPS

We used 11 years of GPS data (2006–2016) from the five Swedish GNSS sites mentioned above. Linear horizontal gradients in the east and the north directions were estimated with a temporal resolution of 5 min. Two GNSS ~~sites~~ stations are operating continuously at the Onsala Space Observatory, on the west coast of Sweden. The primary ~~site~~station, ONSA, was established already in 1987 and the other ~~site~~station, ONS1, was taken into operation in 2011. The six antenna ~~sites~~ installations are shown in Figure 3. The antennas of ONSA and ONS1 are located within 100 m from each other and should observe almost identical

Table 1. Summary of used datasets.

Dataset [1]	Resolution	Time period	ONS1	ONSA	SPT0	VIS0	MAR6	KIR0
GPS (10) [a]	5 min	2006–2016	–	√	√	√	√	√
GPS (10) ECMWF [b]	5 min 6 h	2013–2016 2006–2016	√	√	– √	– √	– √	– √
GPS (20) [c]	5 min	2013–2016	√	√	–	–	–	–
WVR	15 min	2013–2016	√	√	–	–	–	–
VLBI	6 h	6–20 May 2014	√	√	–	–	–	–
ECMWF [2] 6 h 2006–2016 √ √ √ √ √ √ height								

[a] The GPS data were processed with elevation cutoff angles equal to 10°.

[b] (Boehm and Schuh, 2007)

[c] The GPS data were processed with elevation cutoff angles equal to 3°, 10°, and 20°, different mapping functions, and elevation angle dependent weighting.

atmospheric gradients. For the time period 2013–2016 we compare gradients from these two sites stations with simultaneously estimated gradients using data from a WVR.

The analysis of the GPS data follows the same lines as described by Ning et al. (2013) and is summarised in Table 2. Specifically we mention that each day is analysed independently after adding 3 h of data from the previous day and 3 h from the following day, i.e. in total 30 h. The reason is to avoid discontinuities at midnight in the estimated time series.

Recent work by Kačmařík et al. (2018) compared estimated gradients with those from a numerical weather model using different gradient mapping functions and elevation cutoff angles. They found the best agreement for an elevation cutoff angle equal to 3°. They also showed that the Bar-Sever et al. (1998) gradient mapping function resulted in 17 % smaller gradient amplitudes compared to the Chen and Herring (1997) mapping function. For the 11-year study presented in the next section we use a 10° elevation cutoff angle only, whereas we use several different elevation cutoff angles in the comparison with the WVR data from the Onsala site for a 4-year period.

Based on the five-minute gradients we calculated mean values over 15 min, 1 h, 6 h, 1 day, and 1 month in order to match the temporal resolution of the comparison data and to study the variability of the wet and the hydrostatic gradients over different time scales.

An example Examples of the sky coverage of the GPS observations is are shown in Figure 4 for the Onsala site. At this latitude there is a significant part of the sky that is never sampled, just north of the zenith direction. It is reasonable to assume that this will have a negative impact on the estimated gradients, and especially in the north direction.

Figure 3. The six antenna installations used to acquire the GPS data. See Figure 2 for their geographical location.

Table 2. Processing of GPS data.

Parameter	Description / Value
Processing software	GIPSY v6.2 (Webb and Zumberge, 1993)
Strategy	Precise Point Positioning (Zumberge et al., 1997) final orbit and clock products
~~Mapping function~~	were provided by JPL obtained from the legacy GIPSY-OASIS software[a]
Reference frame	IGS08
Mapping functions for ΔL_z	Vienna 1 2006 (VMF1) (Boehm et al., 2006)[b]
Mapping function for Ξ	Bar-Sever et al. (1998)
Elevation cutoff angle	10° ~~or 20~~[c]
Zenith delay	Estimated every 5 min, constraint 10 mm/$\sqrt{\text{h}}$ (Jarlemark et al., 1998)
Linear horizontal gradient	Estimated every 5 min, constraint 0.3 mm/$\sqrt{\text{h}}$ (Bar-Sever et al., 1998)
Ocean tide model	FES2004 (Lyard et al. , 2006)
Antenna phase centre	~~igs~~igs08_1740.atx (Schmid et al., 2007)[d]
Ambiguity resolution	Yes (Bertiger et al., 2010)
Ionosphere model	2nd order (IGRF)~~[1]~~[e] (Matteo and Morton, 2011)

[a] For the 11-year data set, for the 4-year data set, the products were obtained from a new GipsyX software. We noted that the difference in the products due to the change of software is small (Sibois et al., 2017).

[b] For the 11-year data set, for the 4-year data set also the weighted VMF1 and the NMF (Niell, 1996) were used.

[c] For the 11-year data set, for the 4-year data set also 3° and 20° were used.

[d] For the 11-year data set, for the 4-year data set igs08_1869.atx were used.

[e] International Geomagnetic Reference Field

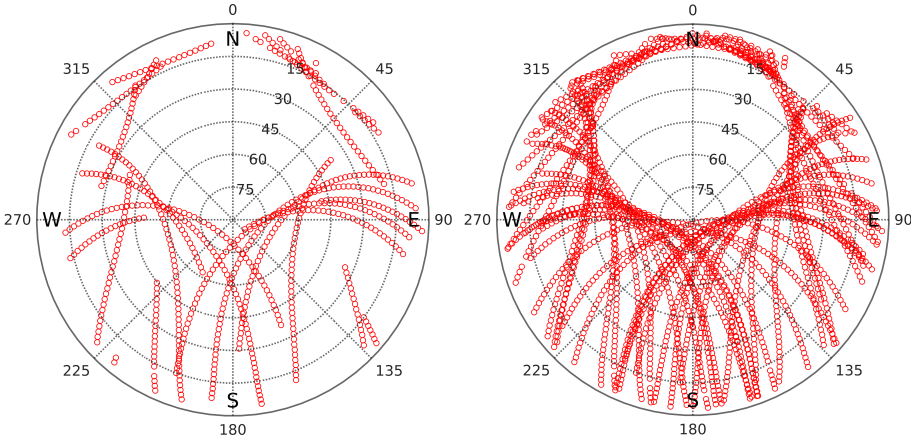

Figure 4. Sky ~~plot~~ plots of GPS observations from 6 to 12 UT (left) and from 0 to 24 UT (right) on May 12, 2014. This particular day was chosen because results from this day are discussed in Section 5.2. The sky distribution of observations is very similar, although not identical, for all days.

Figure 5. The water vapour radiometer (WVR) Konrad at the Onsala Space Observatory.

3.2 Microwave radiometer

The microwave radiometer, shown in Figure 5, is designed in order to provide independent estimates of the wet propagation delays for space geodetic applications. It measures the emission from the sky, on and off the water vapour line at 22.2 GHz. Its specifications are summarised in Table 3 and the data processing is carried out as is described for another WVR by Elgered and Jarlemark (1998).

During the time period 2013–2016 the WVR was observing in a sky mapping mode as is illustrated in Figure 6. A disadvantage of a WVR is that the algorithm for calculation of the wet propagation delay ~~breaks down~~ fails for data acquired during rain or when large liquid drops are present in the sensed atmosphere. Typically such conditions imply large positive errors in the wet delay, and the water vapour content (Westwater and Guiraud, 1980). Therefore, data taken during rain, or when the estimated equivalent amount of liquid water in the zenith direction is >0.7 mm, are discarded from the gradient analysis. In addition there are also time periods when the WVR hardware has failed. The amount of analysed data are shown in Figure 7 as the number of individual observations per day. The first long data gap, in 2014–2015, was caused by a broken mechanical waveguide switch and the second long gap, in 2015–2016, was due to broken cables in the so called cable wrap. The cable wrap was redesigned.

The WVR gradients are estimated based on all observations carried out during a period of 15 min ~~period~~ using the method of least squares. We used the so called four-parameter model, fitting a zenith wet delay (ZWD), a ZWD rate, and an east and a north linear horizontal gradient to the data (Davis et al., 1993). This means that the estimated gradients are independent of the adjacent estimates, which is different from the gradients estimated from the space geodetic techniques, where ~~constraints with time~~ temporal constraints are applied.

Table 3. Specifications for the Konrad WVR.

Parameter	Value
Frequencies	20.6 GHz and 31.6 GHz
Antenna type (one for each channel)	Conical horn with lens
Antenna beam FWHM[1][a], E-plane, ch.1 / ch.2	2.9° / 2.0°
Antenna beam FWHM[1][a], H-plane, ch.1 / ch.2	3.4° / 2.3°
Reference temperatures (both channels)	313 and 373 K
System noise temperatures, channel 1 / 2	450 / 550 K
RF bandwidth (double sideband)	320 MHz (both channels)
Absolute accuracy (weather dependent due to the quality of tip curves)	1–3 K
Repeatability	0.1 K

[a] FWHM = Full Width Half Maximum

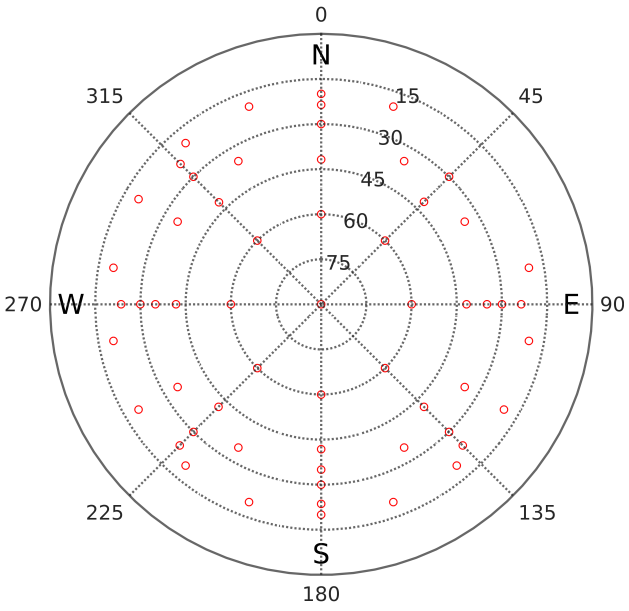

Figure 6. A measurement cycle ~~with~~ of the WVR begins with two azimuth scans. In order to avoid emission from the ground the lowest elevation angle observed is 20°. Starting in the north, first at an elevation angle of 20° clockwise to the north (excluding the azimuth angles of 40° and 60° due to a nearby radio telescope), and then counterclockwise at an elevation angle of 35°. Thereafter four tip curves are made over the zenith direction (implying ~~that~~ four observations ~~are made~~ in the zenith direction during each cycle): from the north to the south, from the southwest to the northeast, from the east to the west, and from the northwest to the southeast. The cycle is about 8 min long and is repeated continuously, implying that almost two complete cycles are executed during the time of the ~~highest~~ temporal resolution used when estimating gradients, i.e. 15 min.

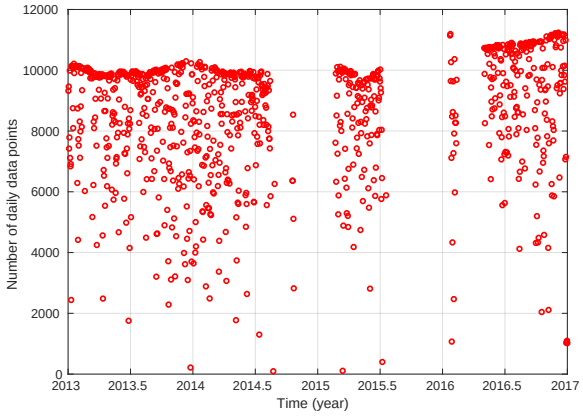

Figure 7. Number of data points per day observed by the WVR. During days without data loss, e.g. due to rain, each estimated gradient is based on approximately 100 observations in the directions illustrated in Figure 6. Observations close to the sun are removed from the raw data before the data analysis is carried out which causes the seasonal variation in the maximum number of observations per day. During the last year the measurement cycle was optimised by reducing some of the time delays inserted between samples but the observational sequence shown in Figure 6 was used during the whole period.

3.3 ~~ECMWF data~~

~~The Technical University of Vienna provides horizontal hydrostatic and wet gradients based on ECMWF data for many space geodetic sites globally. Figure 2 depicts the five sites used here. Details are given by Boehm and Schuh (2007), so we just mention the characteristics that are most relevant for our comparisons. Of importance to us is the temporal resolution of 6 h, which implies that the short term variability in the water vapour will be averaged out. We anticipate, however, that these data are useful to separate the hydrostatic delay gradients from the total delay gradients estimated from the GNSS data. The data are available during certain time periods from the mid of 2005 and are more continuous from 2006. We decided to use the data from 2006 to 2016, resulting in a time series of 11 years.~~

3.3 Very long baseline interferometry data

We have used the VLBI data from the CONT14 campaign coordinated by the International VLBI Service (Nothnagel et al., 2017). The IVS organises continuous (CONT) VLBI campaigns every third year in order to acquire state-of-the-art VLBI data over a time period of two weeks and to demonstrate the highest accuracy of which the current VLBI system is capable. The primary goal of these CONT campaigns is to support research concerning high resolution Earth rotation (Haas et al., 2017) reference frame stability, and daily to sub-daily site motions, but also other aspects. A concise overview of the IVS CONT campaigns is given by MacMillan (2017).

The CONT14 campaign was observed during May 6–20, 2014. The VLBI data were analysed with the calc/solve VLBI data analysis software (Ma et al., 1990). Station positions, ZWD, atmospheric horizontal gradients, relative clock parameters w.r.t. a reference station, as well as earth rotation parameters were estimated. The relative clock parameters were estimated as ~~piece-wise linear offsets~~ a piecewise linear continuous function every hour, with a constraint of ~~5.0^{-14}~~ $5 \cdot 10^{-14}$ s/s between clock rate segments. The ZWD and atmospheric gradients were estimated as ~~piece-wise linear offsets~~ piecewise linear continuous functions (i.e. not stochastic processes) with a temporal resolution of 30 min and 6 h, respectively. Constraints for the variability of 15 mm/h ~~between~~ for the ZWD rate segments, ~~0.5 mm for gradient offsets~~ and 2 mm/day for gradient rates were applied. The NMF (Niell, 1996) mapping functions for ZWD and the Chen and Herring (1997) mapping function for gradients were used in the analysis, together with meteorological information recorded at the VLBI stations. An elevation cutoff angle of 5 degrees was used, and no elevation-dependent weighting.

Figure 8 depicts the sampling of the sky for a 6 h period, which is the highest temporal resolution of the gradient estimates from VLBI, as well as all observations scheduled for a 24 h experiment. This schedule was repeated every day with only minor modifications.

3.4 ECMWF data

The Technical University of Vienna provides horizontal hydrostatic and wet gradients based on ECMWF data for many space geodetic sites globally. Figure 2 depicts the five sites used here. Details are given by Boehm and Schuh (2007), so we just mention the characteristics that are most relevant for our comparisons. ECMWF provide profiles of hydrostatic and wet

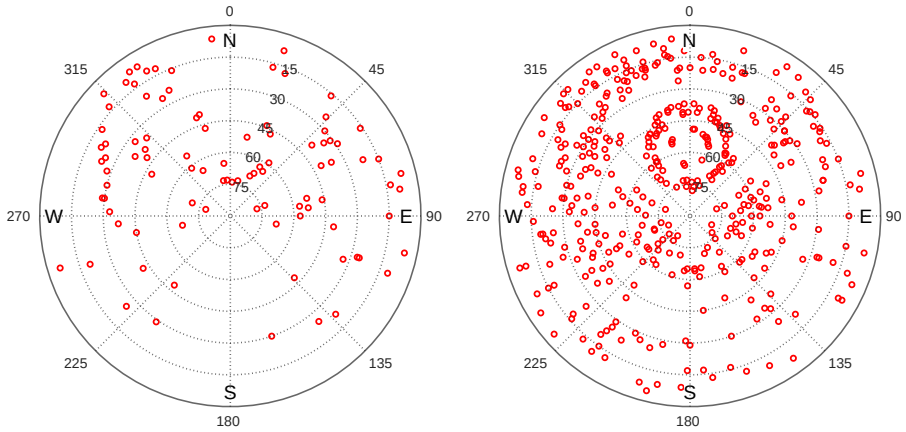

Figure 8. The directions of the VLBI observations for the time period from 6 to 12 UT (left) and from 0 to 24 UT (right), both on May 12, 2014.

refractivities with a temporal resolution of 6 h, and a spatial resolution of 0.25° (∼30 km). The profile closest to the site are used together with one profile to the east and one profile to the north to calculate the refractivity gradient profiles. These are thereafter integrated using Eq. (5) to give the integrated horizontal delay gradients. The data are available during certain time periods from the mid of 2005 and are more continuous from 2006. We decided to use the data from 2006 to 2016, resulting in a time series of 11 years.

As an introduction to the results, presented in the following sections, examples of the ECMWF hydrostatic and wet gradients are illustrated in Figure 9. Worth noting may be that the wet gradients dominate for the temporal resolution of 6 h, whereas the wet and the hydrostatic gradients show similar standard deviations (SD) for the monthly averages.

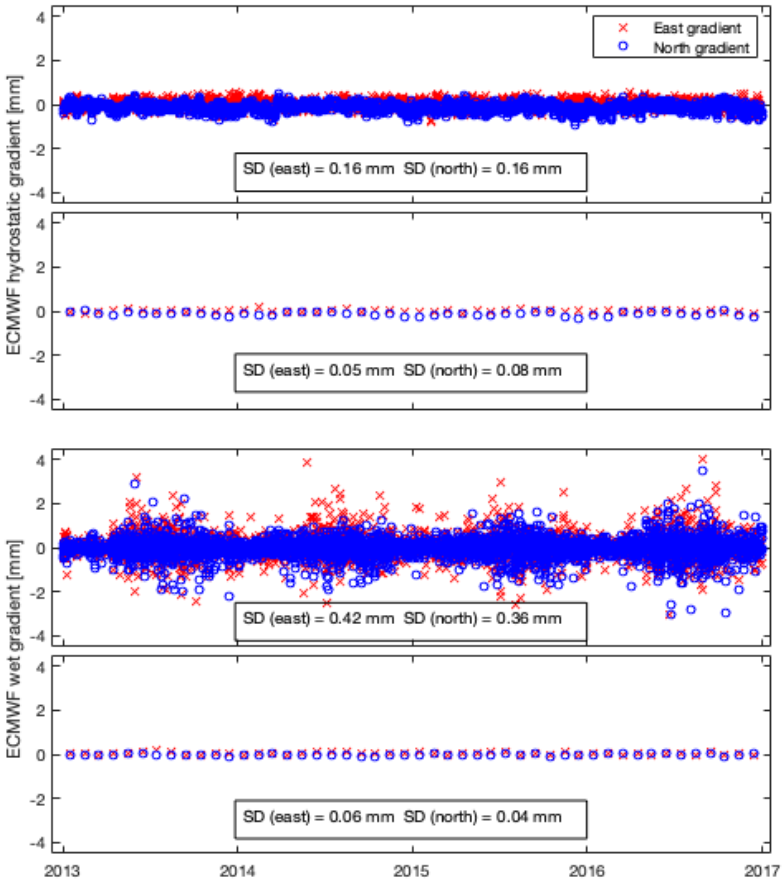

Figure 9. The ECMWF gradients for the Onsala (ONSA) site during the 4-year time period studied in Section 5. From the top: hydrostatic gradients every 6 h, their monthly averages, wet gradients every 6 h, and their monthly averages.

4 Comparison of gradients from GPS and ECMWF data 2006–2016

4.1 Seasonal variations of horizontal gradients

We start by investigating the characteristics of the gradients over the year. In Figure 10 we present the monthly mean gradients for the time period 2006–2016 estimated from ECMWF data and GPS data from the Onsala (ONSA) ~~site~~station.

We can clearly see negative north ~~gradient~~ gradients in the winter, with a mean value around −0.2 mm, both in the GPS and the ECMWF results. When the ECMWF gradients are separated into the hydrostatic and the wet components this variation appears in the hydrostatic component. We interpret this effect as the influence of the Icelandic low pressure system ~~(Hewson and Longley, 1944)~~mentioned in Section 2. Another feature is seen in the ECMWF wet gradients. They are larger in the summer when the wet refractivity is higher, and, at least according to the ECMWF data, there is a tendency to a positive east gradient in the summer. The ONSA GPS ~~site~~ station is located a few hundred metres from the coastline, suggesting that the air on the average is more humid over land compared to over the sea~~in the ECMWF model~~. A possible cause could be the sea breeze that occurs during the summer (Craig et al., 1945; Miller et al., 2003). The issue of wet gradients is studied further using a higher temporal resolution and comparisons with the WVR data in Section 5.1.

The results for the other four ~~sites~~ stations (KIR0, MAR6, SPT0, and VIS0) show identical systematic features except KIR0, which is at a higher latitude and ~~is less humid~~ has a less humid climate. At KIR0 the average monthly wet gradients are insignificant except during the summer months. Furthermore, the influence of the Icelandic low pressure in the winter is not as large as it is at the other four ~~sites~~stations.

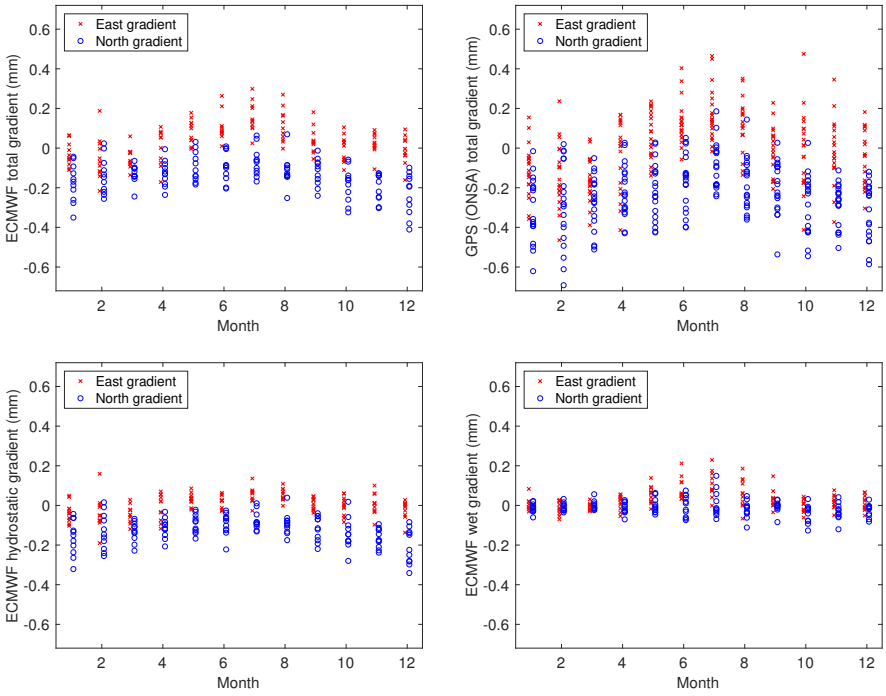

Figure 10. Monthly means of estimated gradients at the Onsala ~~site~~ station for the period 2006–2016. The top graphs show the total gradients from ECMWF (left) and GPS (right). The graphs at the bottom show the ECMWF gradients when separated into the hydrostatic (left) and the wet gradient (right).

Table 4. Correlation coefficients for the total east and north linear horizontal gradients estimated from GPS data and compared to ECMWF data.

~~Site~~ Station	~~Hourly~~ Six hourly		Daily		Monthly	
	East	North	East	North	East	North
Kiruna (KIR0)	0.55	0.53	0.76	0.75	0.77	0.82
Mårtsbo (MAR6)	0.58	0.51	0.75	0.72	0.83	0.80
~~Onsala (ONSA) 0.60 0.60 0.75 0.78 0.90 0.90~~ Borås (SPT0)	0.58	0.58	0.74	0.74	0.88	0.85
Visby (VIS0)	0.55	0.56	0.71	0.75	0.84	0.81
Onsala (ONSA)	0.60	0.60	0.75	0.78	0.90	0.90

4.2 Comparing GPS and ECMWF gradients over different time scales at the five ~~sites~~stations

We assess the data quality, in terms of correlation coefficients, between the total GPS and ECMWF gradients estimated at the 5 GPS ~~sites~~ stations using data from 2006 to 2016. These are shown in Table 4.

The correlations seen in all cases confirm that an atmospheric signal in terms of linear gradients is detected by the GPS observations. We note that the correlation coefficients increase for longer averaging time periods. Our interpretation is that by long term averaging we compare a larger fraction of the gradient that is caused by large scale temperature and pressure gradients, which is better modelled by the ECMWF data. Unfortunately, the temporal resolution of 6 h in the ECMWF data is not sufficient to resolve neither rapid changes in the pressure related to moving weather systems nor many of the short lived small-scale gradients associated with the variability in the water vapour.

Another result worth noting is that the two ~~sites~~ stations with the highest correlation coefficients, ~~and~~ especially for the monthly averages, are ONSA and SPT0. These two ~~sites~~ stations are the only ones that are equipped with microwave absorbing material below the antenna and above the metal plate used for the antenna mounting. This could reduce the impact from unwanted multipath effects. The phenomenon calls for further studies.

Assuming that the ECMWF hydrostatic gradients ~~, linearly interpolated between the 6 h values,~~ are reasonably accurate we have the possibility to subtract this hydrostatic gradient from the estimated total GPS gradient in order to compare the wet gradients at these five ~~sites~~stations. In Table 5 we present the mean values and the standard deviation of these for the three different temporal resolutions. ~~We note that when the wet gradients are averaged over one hour and one day,~~ For the 6-hour temporal resolution the GPS gradients estimated at the same time epoch as the ECMWF gradients are compared. The daily and monthly values are averages using all availiable data. We note that the standard deviations (SD) for the wet gradients obtained for the KIR0 ~~site~~ station for 6 h and one day are significantly smaller. This is likely a consequence of the lower humidity at the ~~site~~station. For monthly averages, however, all ~~sites~~ stations have comparable SD, indicating that at this ~~low~~ level other effects, e.g. instrumental, become important.

Table 5. Mean values and standard deviations (SD) over the 11 years of estimated horizontal wet gradients from GPS data for different temporal resolutions.

~~Site~~ Station	ZWD[1] [a]		Horizontal gradient				
			Mean[2] [b]		~~Hourly~~ Six hourly SD		D
	Mean (mm)	SD (mm)	East (mm)	North (mm)	East (mm)	North (mm)	Eas (mm
Kiruna (KIR0)	61	36	−0.20	−0.02	0.41	0.43	0.2
Mårtsbo (MAR6)	88	46	−0.22	−0.02	0.50	0.53	0.3
~~Onsala (ONSA) 92 47 −0.01 −0.08 0.54 0.50 0.32 0.30 0.13 0.10~~ Borås (SPT0)	87	45	−0.06	−0.12	0.50	0.49	0.3
Visby (VIS0)	88	47	−0.06	−0.10	0.55	0.51	0.3
Onsala (ONSA)	92	47	0.01	−0.08	0.54	0.50	0.3

[a] The Zenith Wet Delay (ZWD) is included to illustrate the amount of water vapour in the atmosphere above the station.

[b] The mean gradient values are based on the 6 h gradients.

4.3 Long term trends

Given that horizontal gradients in general are small and that the larger values typically occur for a short time we expect that any long-term trends would be very small and therefore also difficult to detect. An estimated gradient has a direction and from a time series we estimate trends for the east and the north gradients. Combining ~~these two trends~~ the east and north gradients offers the possibility to also search for trends in the total amplitude value of the gradient ~~at the site~~ $\left(\sqrt{\Xi_e^2 + \Xi_n^2}\right)$ at the station. A positive trend in the ~~amplitude will~~ total amplitude can also occur if there is an increase in the variability at the ~~site~~station, which can happen even if there ~~are~~ is no trend, neither in the east, nor in the north ~~gradients~~gradient. For these five ~~sites~~ stations we have estimated linear gradients in the east and the north direction as well as for the total gradient amplitudes over the 11 years. The trends are indeed very small~~. Typically they are all~~ , typically well below 0.01 mm/year. The highest value is −0.02 mm/year for the wet gradient in the north direction at the SPT0 ~~site~~station. If this trend originates from the atmosphere it is a local effect because it is 6 times as large as the wet north gradient trend at the nearby ONSA ~~site. On the other hand we cannot rule out that it is an effect due to a not~~ station. A typical formal 1-sigma uncertainty of 0.01 mm/year is obtained if we assume that the deviations from the model is white noise, but 0.04 mm/year is estimated by taking the short term temporal correlation of the deviations into account using the model presented by *Nilsson and Elgered* (2008). In addition to that the estimated trends are small relative to their uncertainties we cannot assume perfectly stable hardware at the ~~site, although it is far from as dramatic as the problems~~ station. For example, hardware problems giving a large impact on the estimated gradients have been reported by Douša et al. (2017). Given these circumstances it seems unlikely to detect any trends in gradients caused by the atmosphere unless there is a dramatic local effect of the weather conditions at the site.

5 Gradients at the Onsala site

5.1 Wet gradients from GPS and WVR

For the Onsala site we have total gradients from the two GPS ~~sites~~stations, hydrostatic and wet gradients from ECMWF, and wet gradients from the WVR ~~. First we compare the total gradients~~ for the time period 2013–2016. Gradients in the east and the north ~~direction~~ directions are estimated from the GPS data for five different solutions. We use three different elevation cutoff angles for the VMF1 zenith delay mapping functions. One additional solution is carried out with elevation dependent weighting ($\sin(\varepsilon)$) and in the fifth solution the VMF1 mapping functions are replaced by the NMF. As stated earlier the gradient mapping function presented by Bar-Sever et al. (1998) is used in all cases. ~~A comparison is shown in Figure 12. We expect that the two GPS sites share several error sources and therefore there is a significant common mode suppression of errors, meaning that the rather high correlation may be slightly overoptimistic.~~

~~Correlations between estimated total gradients from the GPS sites ONSA and ONS1 using all data from the period 2013–2016.~~

~~In order to compare the wet gradients~~ When we use the independent WVR data to assess the quality of the gradients estimated for ONSA and ONS1, the hydrostatic gradients from ECMWF (see Figure 9), linearly interpolated to match the time epochs of the GPS gradients, are subtracted from the estimated total GPS gradients. Thereafter we form 15 min averages for the east and the north wet gradients from GPS and compare to the corresponding WVR results. ~~Correlation plots are~~ An overview of the data is presented in Figure 11 in terms of monthly means of total gradient size and ZWD. The GPS solution is the one with a 3° elevation cutoff angle, no weighting, and the VMF1 mapping functions. Here we note that the WVR gives much larger gradients. This depends mainly on that no constraints are applied in the WVR data analysis. The WVR gradients for one 15-minute period do not depend on earlier or later estimates. The WVR is also less of an all weather instrument, being sensitive to liquid water in the sensed atmosphere. This is likely the cause for positive systematic errors in the ZWD as well as occasional overestimates of gradient amplitudes. In this context the 17 % difference in gradient amplitude depending on mapping function used reported by Kačmařík et al. (2018) is less critical. The uncertainty of the estimated gradient amplitude, to which the assumption of a linear model for the atmosphere is also contributing, is significantly larger.

The results for the different GPS solutions are summarised in Tables 6 and 7. Because of the different gradient amplitudes from the WVR and GPS, we present mean values and SD of the differences as well as correlations coefficients. Table 6 shows the results when the total gradients from the stations ONSA and ONS1 are compared to each other. Table 7 shows the results when the wet gradients from ONSA and ONS1 are compared to the WVR gradients. We note that in both tables the best agreement between the gradients estimated is obtained for an elevation cutoff angle equal to 3°. This confirms the results presented by Kačmařík et al. (2018) using a GNSS station network in central Europe. This result was not expected by us, given that the WVR has an elevation cutoff angle of 20° (in order to avoid ground-noise pickup) the GPS solution using the same cutoff angle would show a better agreement. One interpretation of this result is that for the temporal resolutions of 5–15 min the low elevation observations are important in order to distinguish the gradient parameters relative to other estimated parameters

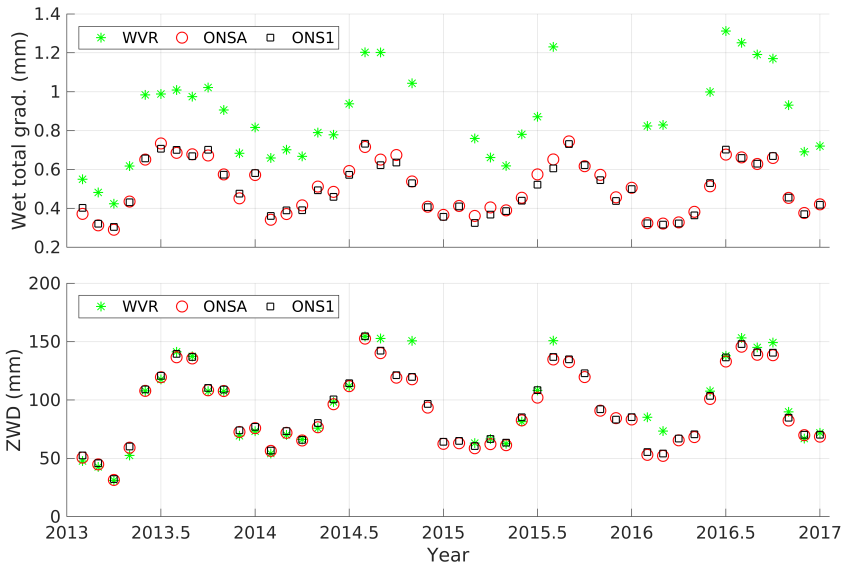

Figure 11. Time series of monthly means of wet total gradients, $\sqrt{\Xi^2_{e,wet} + \Xi^2_{n,wet}}$ (top) and ZWD (bottom) from GPS and WVR. When forming monthly means the correlation coefficients become high. The total wet gradients: WVR vs. ONSA/ONS1 are both 0.85 and ONSA-ONS1 is 0.99. For the ZWD: WVR vs. ONSA/ONS1 are both 0.97 and ONSA-ONS1 is 0.999. When correlating the wet total gradients with the ZWD we obtain 0.95 for the WVR, 0.93 for ONSA and 0.92 for ONS1.

in the GPS analysis. A higher elevation cutoff angle will remove many observations towards the north, and especially for a cutoff angle of 20°, see Figure 4.

The solution giving the best agreement, when comparing gradients from ONSA and ONS1 data with each other, is the one with elevation dependent weighting, whereas the comparisons with the WVR, for both ONSA and ONS1 give the best agreement without weighting. Since the WVR provides independent gradients, we will in the following focus on the VMF 3° solution without elevation dependent weighting.

A correlation plot for the VMF1 solution with a 3° elevation cutoff angle is shown in Figure ~~13.~~ 12. As in the previous section we see a slightly higher correlation for the east gradients, possibly because of the poorer sampling on the sky north of the zenith direction due to the geometry of the GPS satellite constellation at this latitude (see Figure 4).

The two GPS stations share several error sources, such as clock and orbit errors of the observed satellites, and the use of the same mapping functions, meaning that the rather high correlation is overoptimistic due to a common mode suppression of errors.

Correlation plots for the wet gradients from ONSA, ONS1, and the WVR are presented in Figure 13. As expected, the correlations between the estimated gradients from the two GPS ~~sites~~ stations are significantly higher compared to when the GPS gradients are correlated with the gradients from the WVR. It is also not surprising that the correlation between wet gradients from ONSA and ONS1 are slightly lower compared to the correlation between the total gradients (Figure 12). When subtract-

Table 6. Assessment of the different GPS solutions comparing results from the two GPS stations ONSA and ONS1.

GPS Solution	Mean Difference[a]		Standard Deviation		Correlation Coefficient	
	East (mm)	North (mm)	East (mm)	North (mm)	East (mm)	North (mm)
VMF 3°	−0.01	0.03	0.22	0.25	0.91	0.87
VMF 3°[b]	0.03	0.02	0.15	0.16	0.95	0.92
NMF 3°	−0.01	0.05	0.23	0.26	0.91	0.86
VMF 10°	0.02	0.04	0.25	0.27	0.91	0.88
VMF 20°	0.33	0.36	0.39	0.47	0.82	0.70

[a] The mean difference is ONS1−ONSA.

[b] Elevation dependent weighting, $\sin(\varepsilon)$

Table 7. Assessment of the different GPS solutions for the two GPS stations ONSA and ONS1 relative to the WVR data.

GPS Solution	Mean Difference[a]		Standard Deviation		Correlation Coefficient	
	East (mm)	North (mm)	East (mm)	North (mm)	East (mm)	North (mm)
ONSA						
VMF 3°	0.23	−0.07	0.64	0.57	0.68	0.64
VMF 3°[b]	0.21	−0.06	0.71	0.62	0.58	0.55
NMF 3°	0.22	−0.07	0.64	0.57	0.68	0.64
VMF 10°	0.20	−0.10	0.65	0.59	0.66	0.62
VMF 20°	−0.02	−0.28	0.75	0.73	0.54	0.42
ONS1						
VMF 3°	0.22	−0.04	0.64	0.58	0.68	0.64
VMF 3°[b]	0.24	−0.02	0.71	0.63	0.58	0.55
NMF 3°	0.21	−0.02	0.64	0.58	0.68	0.63
VMF 10°	0.22	−0.04	0.66	0.59	0.66	0.62
VMF 20°	0.36	0.15	0.79	0.73	0.49	0.42

[a] The mean difference is the offset referenced to the corresponding WVR time series.

[b] Elevation dependent weighting, $\sin(\varepsilon)$

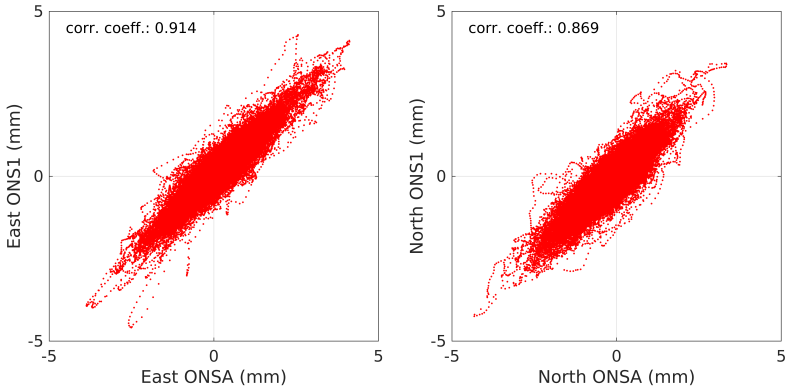

Figure 12. Correlations between estimated ~~wet~~ total gradients from the ~~WVR and the wet gradients from~~ GPS ~~data~~ stations ONSA and ONS1 using all data with a 5 min resolution from the period 2013–2016.

ing the hydrostatic gradients, a common signal is removed and the dynamic range is reduced, which affects the correlation coefficients. ~~Furthermore, the~~

There are several reasons why the correlation coefficients with the WVR are lower: (1) they do not have common sources of errors; (2) the WVR data suffer both from white noise and algorithm errors, especially when liquid water is present; (3) the WVR data for each 15-minute period are independent of the adjacent periods, whereas there are temporal constraints on the gradients estimated from the GPS data; (4) the sampling on the sky agrees also much better between the two GPS ~~sites~~stations, assuming that in general the directions of the observations are towards the same satellites, whereas the WVR ~~'s~~ observations are evenly spread over the sky and above an elevation angle of 20°.

~~We also note that the correlations are in general higher for the east gradient, possibly because of the poorer sampling on the sky north of the zenith direction due to the geometry of the GPS satellite constellation (see Figure 4). Another issue related to~~ Concerning the sampling of the ~~sky coverage of the observations is that the WVR has an~~ atmosphere, the use of a multi-GNSS constellation has been shown to improve the agreement between GNSS gradients with those estimated from a WVR (Li et al., 2015). In this context it should be noted that with many more GNSS observations the optimum elevation cutoff angle ~~of 20 degrees in order to avoid ground-noise pickup. Therefore, we also processed the GPS data with an elevation cutoff angle equal to 20 degrees, expecting that a better agreement between the spatial~~ may not be as low as 3° because of an improved sampling of the ~~WVR and GPS would result in higher correlation coefficients. All the correlation coefficients in Figure 13 were, however, reduced at the order of 10 %. One interpretation of this result is that for the temporal resolution of 15 min the low elevation observations are important in order to distinguish the gradient parameters relative to other estimated parameters in the GPS analysis. Therefore we will not present these results in any more detail.~~ atmosphere.

We investigated if an average of the ~~estimated~~ wet gradients from both GPS stations, ONSA and ONS1, estimated at the same time epoch, will improve the agreement with the WVR. ~~The result is shown in Figure ??. Comparing Figure ?? with~~

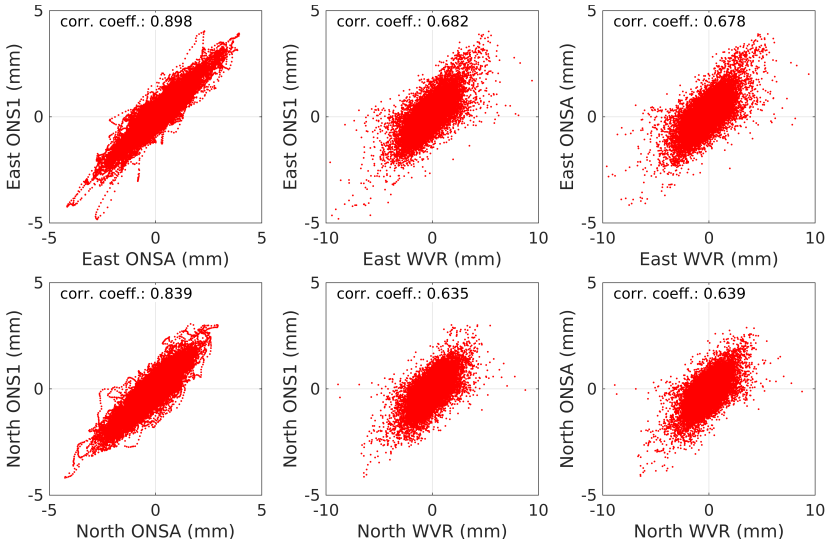

Figure 13. Correlations between estimated wet gradients from the WVR, ONSA and ONS1 using all data from the period 2013–2016. The data in the graphs with ONSA and ONS1 (left) have the original 5 min resolution, whereas the GPS data are averaged over 15 min when compared to the WVR data (middle and right). Note the different scale on the axes for the WVR data. The correlation coefficients obtained when the east gradients from the WVR were correlated with the original total gradients from GPS were 0.633 for ONSA and 0.637 for ONS1. The corresponding values for the north gradients were 0.575 for WVR-ONSA and 0.571 for WVR-ONS1. This supports our assumption that the ECMWF hydrostatic gradients are reasonably accurate when carrying out a linear interpolation between the 6-hour samples.

~~Figure 13 we~~ We see an overall small improvement. For the east gradient the individual ~~correlations~~ correlation coefficients were improved from ~~0.667~~ 0.678 (ONSA) and ~~0.661~~ 0.682 (ONS1) to ~~0.687~~0.698. The corresponding values for the north gradient were ~~from 0.622~~ increased from 0.639 (ONSA) and ~~0.624~~ 0.635 (ONS1) to ~~0.649~~0.666. Our interpretation is that by averaging the GPS gradients from ONSA and ONS1 the stochastic noise is reduced. ~~We identify that the lack of a perfect correlation is due to at least two remaining reasons. One is the systematic effect caused by the different sampling on the sky. The use of a multi-GNSS constellation has been shown to improve the agreement (Li et al., 2015). The other reason is the much higher variability in the time series from the WVR because no temporal constraints are used when estimating these gradients.~~

~~Correlations between the mean values of ONSA and ONS1 wet gradients and the WVR gradients using all data from the period 2013–2016.~~

Correlation plots are shown in Figure 14 for each month of the four years. A clear seasonal dependence is seen, because the variability in the wet refractivity is larger during the warmer time periods, resulting in larger gradients and a larger dynamic range. In ~~a study by~~ Figure 8 of Lu et al. (2016) a correlation coefficient of 0.52 was reported for the months March–May, 2014, between GPS and WVR gradients. Here we show that the variability from month to month is large and therefore the choice of the time period for gradient comparison studies is a critical issue.

Comparing the results obtained for ONSA with those from ONS1 they are almost identical (in both Figures 13 and 14) meaning that in this case there is no obvious improvement from the absorbing material below the antenna on ONSA. This is

different to the previous finding where ONSA and SPT0, with microwave absorbing material, showed a better agreement with ECMWF gradients compared to the KIR0, MAR6, and VIS0 ~~sites~~stations. Our assumption is that the lack of a concrete pillar with a metal mounting plate just below the antenna on ONS1, or any other objects affecting the electromagnetic environment at the antenna, eliminates the need for an absorber (see Figure 3).

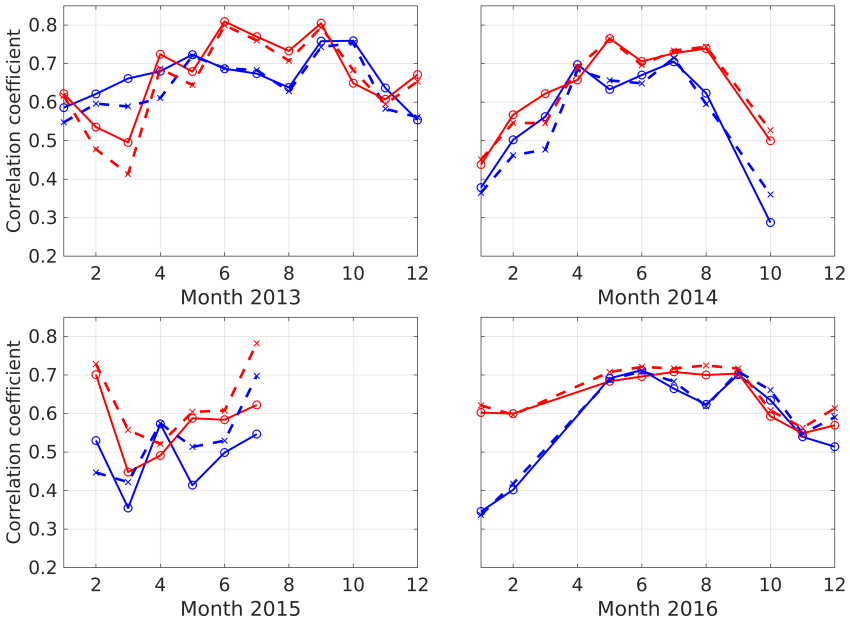

Figure 14. Correlations between estimated wet gradients ~~averaged over 15 min~~ from the WVR data and the ~~different~~ GPS data from ONSA (solid lines) and ONS1 (dotted lines) averaged over 15 min when the hydrostatic gradients have been removed from the total GPS gradients for each month of the four years. The ~~north~~ east gradients are presented with red lines and the ~~east~~ north gradients ~~as black~~ with blue lines. We note that during October 2014 there were problems with the WVR (see Figure 7). During most of the days there is a significant data loss, likely due to rain, which could be the reason for the low correlation during this month.

5.2 ~~Gradients~~ GPS, VLBI, and WVR gradients during ~~the~~ CONT14~~VLBI campaign~~

The total gradients from the two space geodetic techniques GPS and VLBI were compared ~~using the data from~~ to each other and to the WVR during the CONT14 campaign. The GPS gradients were those obtained from the VMF1 solution, unweighted, with a 3° elevation cutoff angle. Observations from several earlier CONT campaigns have been analysed in terms of gradients with different results depending on the ~~site~~ station and the time of the campaign (Teke et al., 2013). ~~Here we focus on GPS and VLBI data from the Onsala site.~~ The estimated time series are shown in Figure 15. ~~Correlation plots~~ The addition of the hydrostatic gradients from ECMWF to the WVR wet gradients did not add any significant variability to the WVR gradients, see Figure 16.

Again we note that the size of the WVR gradients is larger compared to all other instruments. The VLBI gradients correlate with the gradients from the other instruments but their amplitudes are smaller. Given that the sampling of the atmosphere is much more sparse with the VLBI telescope, a short lived gradient in combination with the assumption of linear functions in 6-hour segments, will probably reduce the variability in the estimated amplitude.

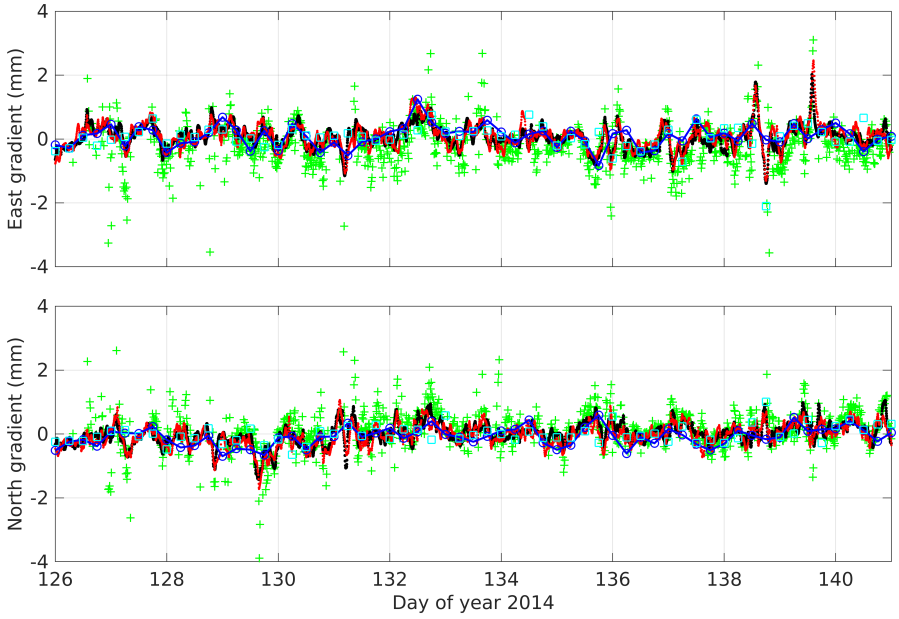

Figure 15. Time series of estimated total gradients during the VLBI CONT14 campaign 6–20 May (days 126–140). The temporal resolution is 6 h for the VLBI gradients (blue circles connect with a solid line), 5 min for the GPS gradients for ONSA (red dots) and ONS1 (black dots), and 15 min for the WVR wet plus the ECMWF hydrostatic gradients (green plus). Also included are the ECMWF total gradients with a 6 h resolution (cyan squares).

Table 8 summarises the correlation coefficients for the east and the north VLBI gradients compared to those from the two GPS ~~sites~~stations, ONSA and ONS1, ~~are presented in Figure ??. We~~ and the WVR. Here we have correlated averages using

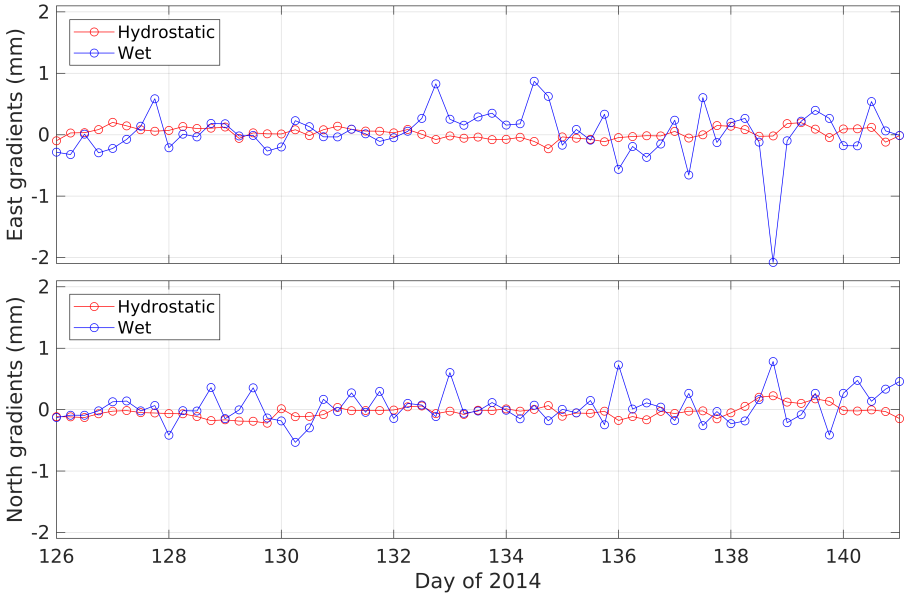

Figure 16. Time series of ECMWF hydrostatic and wet gradients during the CONT14 campaign.

data ±3 h around the VLBI gradient value every 6 h. In order to be consistent also the interpolated data from continuous VLBI segments are averaged in this way.

Again we note that the agreement~~in general~~, in terms of correlation coefficients, is better for the east component compared to the north component. There is a specific example seen in Figure 15 during day 132 (~~May 12~~May 12) where a large north gradient is not detected in the VLBI data. The independent wet gradients obtained from the WVR (~~not shown~~plus the ECMWF hydrostatic gradient) confirm that this gradient was originating from the atmosphere. The left plot in Figure 8 may explain why the north gradient has a larger uncertainty at this specific time.

We attribute the ~~slightly~~ lower correlation coefficients obtained between ~~GPS-VLBI~~ VLBI-GPS and VLBI-WVR using 6 h averages during the CONT14 campaign compared to GPS-WVR 15 min averages for the month of May 2014 in Figure 14 to the sparse sequential sampling of the sky by the VLBI observations. On the other hand, averaging the WVR gradients over ±3 h reduces some of the noise seen in the 15 min values. The future use of the twin telescopes with faster slewing speeds at the site is likely to improve this situation~~which in turn should improve the accuracy~~. During CONT14 there were approximately 360 useful observations at Onsala per day. We expect this to increase by a factor of 6–7 when using the new VLBI Geodetic Observing System (VGOS) (Niell et al., 2018), which means that the use of twin telescopes could result in 200 observations per hour. This in turn makes it possible to improve the temporal resolution of the estimated atmospheric ~~parameters in VLBI experiments.~~ gradients.

Finally, we like to use this 15-day long time series for a discussion on gradient variability. Figure 17 shows the ZWD from the two GPS stations and the WVR. At the end of day 135 more humid air is starting to enter over the site. We note a sudden

Table 8. Comparison of estimated linear gradients from VLBI relative to GPS and WVR data.

Reference Instrument	Mean Difference[a]		Standard Deviation		Correlation Coefficient	
	East (mm)	North (mm)	East (mm)	North (mm)	East (mm)	North (mm)
ONSA	0.01	−0.03	0.22	0.20	0.70	0.69
ONS1	0.03	−0.08	0.22	0.20	0.69	0.67
WVR	0.23	−0.17	0.27	0.27	0.64	0.65

[a] The mean difference is VLBI−reference instrument.

short decrease, followed by a rapid increase. In Figure 5.2 we zoom in on the gradients and the ZWD during this period. Here we have an example where the GPS and WVR gradients occur when different air masses pass over the site. We believe that this example illustrates a situation where GPS/GNSS data in the future can be used to evaluate high resolution numerical weather models.

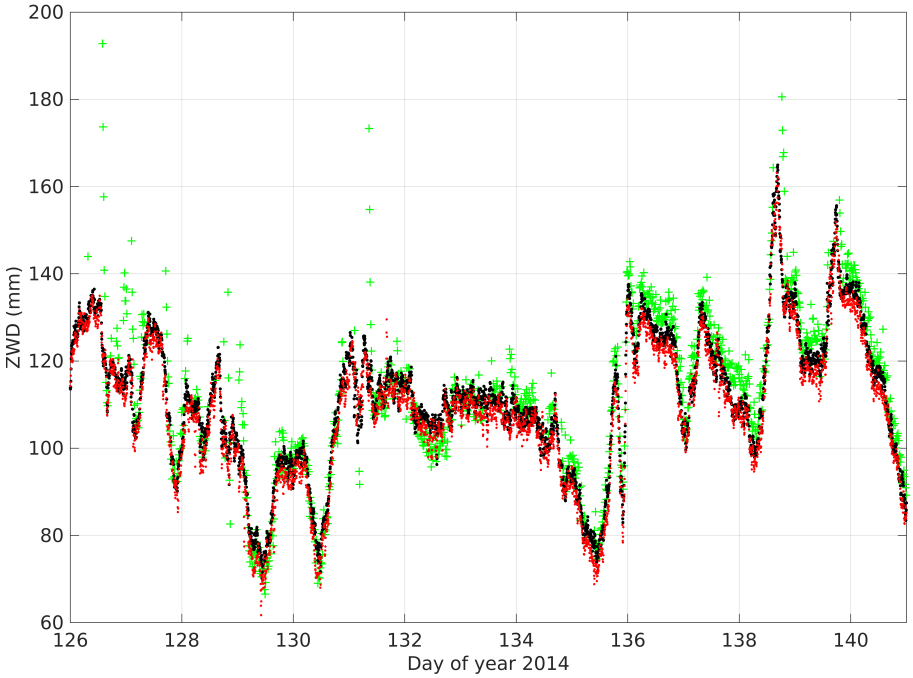

Figure 17. ~~Time series of estimated total east~~ The zenith wet delay (~~top~~ZWD) from ONSA (red dots), ONS1 (black dots), and ~~north~~ WVR (~~bottom~~green plus) during the CONT14 campaign.

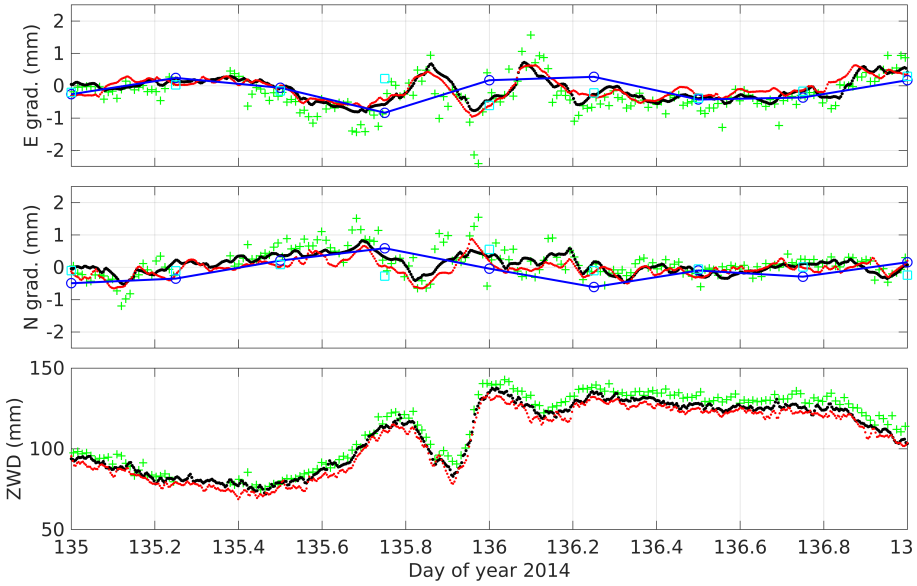

~~Correlation plots of the~~ , ECMWF total ~~estimated VLBI~~ gradients ~~vs the total gradients from the two GPS sites, ONSA and ONS1 during the CONT14 campaign. The red circles are at the epochs of the VLBI estimates, every 6 h, and the black dots are linearly interpolated VLBI results~~ with a ~~temporal resolution of 5~~6 ~~min in order to match the GPS data. The correlation coefficients presented in the graphs are calculated using mean values for the period of ±3~~ h ~~around the time epochs of the VLBI values~~ resolution (~~6h:~~cyan squares).

~~Correlation plots of the~~ , ECMWF total ~~estimated VLBI~~ gradients ~~vs the total gradients from the two GPS sites, ONSA and ONS1 during the CONT14 campaign. The red circles are at the epochs of the VLBI estimates, every 6 h, and the black dots are linearly interpolated VLBI results~~ with a ~~temporal resolution of 5~~6 ~~min in order to match the GPS data. The correlation coefficients presented in the graphs are calculated using mean values for the period of ±3~~ h ~~around the time epochs of the VLBI values~~ resolution (~~6h:~~cyan squares).

Figure 18. Zoom in on the time series with gradients ~~from VLBI~~ in Figure 15 and ~~GPS data~~ZWD in Figure 17. The ~~temporal resolution is 6 h for the~~ symbols are as before: VLBI gradients (blue circles connect with a solid line), ~~5 min for the~~ GPS gradients for ONSA (red dots) and ONS1 (black dots)~~. The VLBI observations include~~ , WVR wet plus the ~~days 126–140~~ ECMWF hydrostatic gradients (~~6–20 May~~green plus)~~.~~

~~Correlation plots of the~~ , ECMWF total ~~estimated VLBI~~ gradients ~~vs the total gradients from the two GPS sites, ONSA and ONS1 during the CONT14 campaign. The red circles are at the epochs of the VLBI estimates, every 6 h, and the black dots are linearly interpolated VLBI results~~ with a ~~temporal resolution of 5~~6 ~~min in order to match the GPS data. The correlation coefficients presented in the graphs are calculated using mean values for the period of ±3~~ h ~~around the time epochs of the VLBI values~~ resolution (~~6h:~~cyan squares).

6 Conclusions

We have shown that estimated linear horizontal gradients from GPS data from five sites in Sweden can be understood based on meteorological phenomena. Averaging gradients in the east and the north direction over one month gives correlation coefficients of up to 0.9 when compared to gradients calculated from meteorological analyses of the ECMWF. Monthly averages of the gradients are dominated by the hydrostatic component.

No significant long-term trends were detected for the horizontal gradients. If small gradient trends are detected in the future we recommend to critically assess if they could be caused by station problems or confirmed by a nearby (or even collocated) station.

When studying gradients averaged over shorter time scales, e.g. 15 min, we find the wet component of the gradients to cause most of the variability. We confirm the result from Kačmařík et al. (2018), that an elevation cutoff angle of 3° implies a better agreement when comparing GPS gradients with those from a WVR, in spite of the fact that the WVR does not observe the atmosphere below elevation angles of 20°. Correlation coefficients between wet gradients ~~from GPS~~ simultaneously estimated from GPS and the WVR data can for specific months reach up to 0.8~~when compared to simultaneously estimated wet gradients from the WVR~~. Based on the four years of results we note a strong seasonal dependence, from 0.3 during months with smaller gradients to 0.8 during months with larger gradients, typically during the warmer, and more humid, part of the year.

In general we also note slightly higher correlation coefficients for the GPS derived gradients in the east compared to the north direction. We interpret this difference to be caused by an inhomogeneous spatial sampling on the sky, which is important when we assume that the model describing linear horizontal gradients has deficiencies. The different sampling on the sky is an important issue for any comparison between different techniques. This question remains unresolved and would have to be studied later.

~~No significant long-term trends were detected for the horizontal gradients. If small gradients trends are detected in the future we recommend to critically assess if they could be caused by station problems or confirmed by a nearby (or even collocated) site.~~ Additional issues that deserves attention in future studies, in addition to similar studies in very different climates, e.g. the tropics, can include multi-GNSS observations. At latitudes similar to those in this study, the use of GNSS satellites with a higher orbit inclination will reduce the part of the sky not sampled by GPS. For VLBI the use of VGOS (twin) telescopes will also dramatically improve the sampling of the atmosphere. When WVR data are used to evaluate gradients from the space geodetic techniques one may consider to also apply different constraints for the temporal variability of these estimates.

Data availability. The input GNSS data, in RINEX format, are available from EUREF, https://igs.bkg.bund.de/dataandproducts/browse. The input VLBI data are available from the IVS, ftp://ivs.bkg.bund.de/pub/vlbi/ivsdata/db/2014/. The ECMWF gradients are accessible from the Technical University of Vienna, http://vmf.geo.tuwien.ac.at/trop_products/GNSS/LHG/. The estimated gradients from GPS, VLBI, and WVR data have been registered and archived archived by the Swedish National Data Service (SND).

Author contributions. Gunnar Elgered coordinated and wrote the major part of the manuscript and together with Tong Ning planned the different GNSS data analyses during the COST Action ES1206. Tong Ning performed the GNSS data analyses, resulting in the estimated horizontal gradients. Peter Forkman and Rüdiger Haas carried out the same task for WVR and VLBI data, respectively. All authors contributed in the writing process, in particular to the sections presenting the results produced by each author and approved the entire manuscript before the submission.

Competing interests. The authors declare that they have no conflict of interest.

Acknowledgements. The map in Figure 2 was produced using the Generic Mapping Tools (Wessel and Smith, 1998).

References

Bar-Sever, Y.-E., Kroger, P. M., and Börjesson, J. A.: Estimating horizontal gradients of tropospheric path delay with a single GPS receiver, J. Geophys. Res., 103(B3), 5019–5035, doi:10.1029/97jb03534, 1998.

Bertiger, W., Desai, S.D., Haines, B., Harvey, N., Moore, A.W., Owen, S., and Weiss, J.P.: Single receiver phase ambiguity resolution with GPS data, J. Geod., 84:327–337, doi:10.1007/s00190-010-0371-9, 2010.

Boehm, J., Werl, B. and Schuh, H.: Troposphere mapping functions for GPS and very long baseline interferometry from European Centre for Medium-Range Weather Forecasts operational analysis data, J. Geophys. Res., 111, B02406, doi:10.1029/2005JB003629, 2006.

Boehm, J. and Schuh, H.: Troposphere gradients from the ECMWF in VLBI analysis, J. Geod., 81:403–408, doi: 10.1007/s00190-007-0144-2, 2007.

Brown, R. A.: A secondary flow model for the planetary boundary layer, J. Atmos. Sci., 27, 742–757, 1970.

Bruyninx, C., Habrich, H., Söhne, W., Kenyeres, A., Stangl, G., and Völksen, C.: Enhancement of the EUREF Permanent Network Services and Products, Geodesy for Planet Earth, IAG Symposia Series, 136, 27–35, doi:10.1007/978-3-642-20338-1_4, 2012.

Chen, G., and Herring, T. A.: Effects of atmospheric azimuthal asymmetry on the analysis of space geodetic data, J. Geophys. Res., 102(B9):20489–20502, doi:10.1029/97JB01739, 1997.

Craig, R. A., I. Katz, I., and P. J. Harney, P. J.: Sea breeze cross sections from pyschrometric measurements, Bull. Am. Meteorol. Soc., 26(10), 405–410, 1945.

Davis, J. L., Herring, T. A., Shapiro, I. I., Rogers, A. E. E., and G. Elgered, Geodesy by radio interferometry: Effects of atmospheric modeling errors on estimates of baseline length, Radio Sci., 20, 1593–1607, doi:10.1029/RS020i006p01593, 1985.

Davis, J. L., Elgered, G., Niell, A. E., and Kuehn, C. E.: Ground-based measurement of gradients in the "wet" radio refractivity of air, Radio Sci., 28(6), 1,003–1,018, doi:10.1029/93RS01917, 1993.

Douša, J., Václavovic, P., Eliaš, M.: Tropospheric products of the second European GNSS reprocessing (1996–2014), Atmos. Meas. Tech., 10:1–19, doi:10.5194/amt-10-1-2017, 2017.

Elgered, G., and Jarlemark, P.O.J.: Ground-Based Microwave Radiometry and Long-Term Observations of Atmospheric Water Vapor, Radio Sci., 33, 707–717, doi:10.1029/98RS00488,1998.

Gradinarsky, L. P., Haas, R., Elgered, G., and Johansson, J. M.: Wet path delay and delay gradients inferred from microwave radiometer, GPS and VLBI observations, Earth Planets Space, 52(10), 695–698, doi:10.1186/BF03352266, 2000.

Haas, R., Hobiger, T., Kurihara S., and Hara, T.: Ultra-rapid earth rotation determination with VLBI during CONT11 and CONT14, Journal of Geod., 91(7), 831–837, doi:10.1007/s00190-016-0974-x2016, 2017.

Hewson, E. W. and Longley, R. W.: Meteorology: Theoretical and Applied, New York, John Wiley & Sons, 1944

IERS Conventions: Gérard Petit and Brian Luzum (eds.). (IERS Technical Note; 36) Frankfurt am Main: Verlag des Bundesamts für Kartographie und Geodäsie, 179 pp., ISBN 3-89888-989-6, 2010.

Jarlemark, P.O.J., Emardson, T.R., and Johansson, J.M.: Wet Delay Variability Calculated from Radiometric Measurements and Its Role in Space Geodetic Parameter Estimation, Radio Sci., 33, 719–730, doi:10.1029/98RS00551, 1998.

Kačmařík, M., Douša, J., Zus, F., Václavovic, P., Balidakis, K., Dick, G., Wickert, J.: Sensitivity of GNSS tropospheric gradients to processing options, Ann. Geophys. Discuss., doi:10.5194/angeo-2018-93, 2018.

Li, X., Zus, F., Lu, C., Ning, T., Dick, G., Ge, M., Wickert, J., and Schuh, H.: Retrieving high-resolution tropospheric gradients from multiconstellation GNSS observations, Geophys. Res. Lett., 42(10), 4173–4181, doi:10.1002/2015GL063856, 2015.

Lu, C., Li, X., Li, Z., Heinkelmann, R., Nilsson, T., Dick, G., Ge, M., and Schuh, H.: GNSS tropospheric gradients with high temporal resolution and their effect on precise positioning, J. Geophys. Res. Atmos., 121, 912–930, doi:10.1002/2015JD024255, 2016.

Lyard F., Lefevre, F., Letellier, T., and Francis, O.: Modelling the global ocean tides: Modern insights from FES2004, Ocean Dyn., 56, 394, doi:10.1007/s10236-006-0086-x, 2006.

Ma C., Sauber J. M., Bell L. J., Clark T. A., Gordon D., Himwich W. E., and Ryan J. W.: Measurement of horizontal motions in Alaska using very long baseline interferometry, J. Geophys. Res., 95, 21991–2011, doi:10.1029/JB095iB13p21991, 1990.

MacMillan, D. S.: EOP and scale from continuous VLBI observing: CONT campaigns to future VGOS networks, J. Geod., 91, doi:10.1007/s00190-017-1003-4, 2017.

Matteo, N. A., and Morton, Y. T.: Ionosphere geomagnetic field: Comparison of IGRF model prediction and satellite measurements ~~1991-2010~~1991–2010, Radio Sci., 46, RS4003, doi:10.1029/2010RS004529, 2011.

Meindl, M., Schaer, S., Hugentobler, U., and Beutler, G.: Tropospheric Gradient Estimation at CODE: Results from Global Solutions, J. Meteorol. Soc. Japan, 82, 331–338, doi:10.2151/jmsj.2004.331, 2004.

~~Munn, R. E.: Descriptive Micrometeorology, Academic Press, New York, 1966.~~

Miller, S. T. K., Keim, B. D. , Talbot, R. W., and Mao, H.: Sea breeze: Structure, forecasting, and impacts, Rev. Geophys., 41(3), 1011, doi:10.1029/2003RG000124, 2003

Niell, A. E.: Global mapping functions for the atmosphere delay at radio wavelengths, J. Geophys. Res., 101(B2), 3227–3246, doi:10.1029/95JB03048, 1996.

Niell, A., Barrett, J., Burns, A., Cappallo, R., Corey, B., Derome, M., C. Eckert, C., Elosegui, P., McWhirter, R., Poirier, M., Rajagopalan, G., Rogers, A., Ruszczyk, C., SooHoo, J., Titus, M., Whitney, A., Behrend, D., Bolotin, S., Gipson, J., Gordon, D., Himwich, E., and Petrachenko, B.: Demonstration of a broadband very long baseline interferometer system: A new instrument for high-precision space geodesy, Radio Sci., 53, doi:10.1029/2018RS006617, 2018.

Nilsson, T., and Elgered, G.: Long-term trends in the atmospheric water vapor content estimated from ground-based GPS data, J. Geophys. Res., 113(D19), D19101, doi:10.1029/2008JD010110, 2008.

Ning, T., Elgered, G., Willén, U., and Johansson, J.M.: Evaluation of the atmospheric water vapor content in a regional climate model using ground-based GPS measurements, J. Geophys. Res., 118, 1–11, doi: 10.1029/2012JD018053, 2013.

Nothnagel, A., Artz, T., Behrend, D. , and Malkin, Z.: International VLBI Service for Geodesy and Astrometry Delivering high-quality products and embarking on observations of the next generation J. Geod., 91, 711–721, doi: 10.1007/s00190-016-0950-5, 2017.

Rüeger, J. M.: Refractive index formula for radio waves, Proc. XXII FIG Int. Congr., April 19–26, 2002.

Sanchez-Franks, A., Hameed, S., and Wilson, R. E.: The Icelandic Low as a Predictor of the Gulf Stream North Wall Position, J. Phys. Oceanography, 46, 3, 817–826, doi:10.1175/JPO-D-14-0244.1, 2016.

Schmid, R., Steigenberger, P., Gendt, G., Ge, M., Rothacher, M.: Generation of a consistent absolute phase center correction model for GPS receiver and satellite antennas, J. Geod., 81, 781–798, doi: 10.1007/s00190-007-0148-y, 2007.

Sibois, A., Amiri, N., Bertiger, W., Miller, M., Murphy, D., Ries, P., Sakamura, C., and Sibthorpe, A.: Ensuring a smooth operational transition from GIPSY-OASIS to GipsyX: product verification and validation overview, poster presented at the IGS Workshop, Paris, France, available from http://www.igs.org/presents/workshop2017, 2017.

Teke, K., Nilsson, T., Böhm, J., Hobiger, T., Steigenberger, P., Garcia-Espada, S., Haas, R., and Willis, P.: Troposphere delays from space geodetic techniques, water vapor radiometers, and numerical weather models over a series of continuous VLBI campaigns, J. Geod., 87, 981–1001, doi: 10.1007/s00190-013-0662-z, 2013.

Thompson, D. W. J., and Wallace, J. M.: The Arctic oscillation signature in the wintertime geopotential height and temperature fields, Geophys. Res. Lett., 25, 1297–1300, doi: 10.1029/98GL00950, 1998.

Webb, F. H. & Zumberge, J. F.: An Introduction to the GIPSY/OASIS-II, JPL Publ., D-11088, Jet Propulsion Laboratory, Pasadena, California, 1993.

Wessel, P. and Smith, W. H. F.: New, improved version of generic mapping tools released, EOS Trans. Amer. Geophys. U., 79(47), 579, doi:10.1029/98EO00426, 1998.

Westwater, E.R., and Guiraud, F.O.: Ground-based microwave radiometric retrieval of precipitable water vapor in presence of clouds with high liquid content, Radio Sci., 15, 947–957, doi:10.1029/RS015i005p00947, 1980.

Zumberge, J. F., Heflin, M. B., Jefferson, D. C., Watkins, M. M., and Webb, F. H.: Precise point positioning for the efficient and robust analysis of GPS data from large networks, J. Geophys. Res., 102, 5005–5017, doi:10.1029/96JB03860, 1997.